NASA Technical Paper 1348

Sonic-Boom Minimization With Nose-Bluntness Relaxation

Christine M. Darden

JANUARY 1979

NASA

NASA Technical Paper 1348

Sonic-Boom Minimization With Nose-Bluntness Relaxation

Christine M. Darden
Langley Research Center
Hampton, Virginia

National Aeronautics
and Space Administration

**Scientific and Technical
Information Office**

1979

SUMMARY

A method which provides sonic-boom-minimizing equivalent area distributions for supersonic cruise conditions is described. This work extends previous analyses to permit relaxation of the extreme nose bluntness which is required by conventional low-boom shapes and includes propagation in a real atmosphere. The procedure provides area distributions which minimize either shock strength or overpressure. The minimizing Whitham F-functions for the pressure signatures are also included.

INTRODUCTION

Sonic-boom levels produced by future generation supersonic transports must be considered if their supersonic flight paths, and thus their economic success, are not to be severely restricted. It is generally believed that the best approach to this problem is to include low-boom constraints early in the design process. The procedure described herein provides this constraint in the form of an equivalent area distribution which depends on the design conditions of aircraft weight (lift) and length, and on cruise Mach number and altitude.

Sonic-boom-minimization studies, by Jones, Seebass, and George for uniform and isothermal atmospheres have been reported in references 1 to 6. These analyses have been extended to a real atmosphere in reference 7. All these studies have indicated that the minimizing area distribution is characterized by a bluntness in the leading portion of the area distribution, i.e., the aircraft nose region. Because extreme nose bluntness produces large drag, a method of relaxing the bluntness requirement is needed to offer the opportunity for compromise between blunt-nose, low-boom and sharp-nose, low-drag configurations.

This analysis extends the work of Seebass and George (ref. 6) and Darden (ref. 7) to include nose-bluntness relaxation. Because questions still remain regarding the type of pressure signature and the level of overpressure which are acceptable, either a minimum-shock or a minimum-overpressure signature may be produced for given cruise conditions and nose length.

This analysis has been incorporated into a computer program which is described in the appendix of this paper.

SYMBOLS

Although values are given in both SI and U.S. Customary Units, the calculations for the investigation were made in U.S. Customary Units.

Notation used in the computer printout is given in parentheses.

A	ray-tube area
A_e	equivalent area
$A_e(l)$	equivalent area at equivalent length l
a	speed of sound
B	slope of rise in F-function (eq. (20))
C	height of F-function at balancing point
C_D	drag coefficient
D	constant in F-function equation
F (F and FTAU)	Whitham F-function
G	area of F-function to front balance point
H	height of spike in F-function
h (Z)	airplane altitude
I	impulse of pressure signature, $\int_{P>0} P\,dt$
K (RFK)	reflection factor
l (L)	equivalent length of airplane
M	Mach number
P	pressure perturbation
p	ambient pressure
Δp (Delta P)	overpressure
S	slope of balancing line
t	time
u	speed
V	total area, $\beta W/\rho u^2$
W (WG)	airplane weight
$\tilde{w}$ (W-TILDE)	weight parameter, $\dfrac{V}{B(l - y_f)^{5/2}}$

x,y axial distances

y_f (YF) width of forward spike in F-function

y_r (T) position of rear area balancing

z (r) vertical distance of signal from airplane axis

α advance of acoustic rays

β $= (M^2 - 1)^{1/2}$

βz (BR) shifting factor for axial position

γ ratio of specific heats, 1.4 for air

Γ $= \dfrac{\gamma + 1}{2}$

δ Dirac delta function

η fraction of balancing line slope used in defining F-function

λ (LAM) axial position at which F-function becomes negative

μ Mach angle, $\sin^{-1} \dfrac{1}{M}$

ξ dummy integration variable

ρ density

Subscripts:

a ambient

f front shock

g ground

h altitude of initial waveform

o minimum-overpressure signature

r rear shock

s minimum-shock signature

y axial position

yf axial position of front area, balance

z vertical distance of signal from airplane axis

First and second derivatives with respect to distance are denoted by single and double primes, respectively.

BACKGROUND

Sonic-boom-minimization studies are based primarily on currently accepted sonic-boom prediction methods. These methods, outlined in figure 1, are extensions of work done by Whitham (ref. 8), Walkden (ref. 9), and Hayes (ref. 10). From the complex aircraft configuration and its lift distribution, an equivalent area distribution is defined. This equivalent area distribution then defines the Whitham "F-function" through the following integral relation:

$$F(y) = \frac{1}{2\pi} \int_0^y \frac{A_e''}{(y - \xi)^{1/2}} d\xi \qquad (1)$$

This F-function represents a distribution of sources which causes the same disturbances as the aircraft at some distance from the aircraft.

Because the pressure signal propagates at the local speed of sound, and each point of the signal advances according to its amplitude, the signal is distorted at the ground and, theoretically, can be multivalued. The physically unrealistic multiple values of pressure are, however, eliminated by the introduction of shocks. Shock location, based on the observation that for weak disturbances the shock bisects the angle between two merging characteristic lines, is determined by a balancing of the signature areas within loops on either side of the shocks. This procedure is demonstrated by the shaded areas of the distorted signal in figure 1.

For present-day supersonic aircraft, the propagation distance (altitude) and the pattern of shock coalescence have been such that, at ground level, only two shocks remain in the signature. These two shocks have a linear pressure variation between them (as seen in fig. 2), thus the name "far-field N-wave." For this wave, the shape of the generating aircraft has an effect on the magnitude but no effect on the shape of the resulting signature. For a sufficiently long and slender aircraft, it was found that the ground wave form may possibly not have attained its N-shape remaining instead a mid-field wave. Because the shape of the aircraft does influence the shape of a mid-field pressure signature, aircraft shaping has now become a powerful tool in reducing the sonic boom.

The F-functions for the lower bound of an N-wave (refs. 1 and 2) and for the lower bound of the bow shock in a mid-field signature (refs. 3 and 4) led to the form of the minimizing F-function assumed by Seebass and George for the entire signature. Lung (ref. 11) later proved this to be the minimizing form by "bang-bang" control theory.

Common to all of these minimizing forms of the F-function is a Dirac delta function at $y = 0$. This infinite impulse corresponds to an infinite gradient at the nose of the equivalent area distribution. Aircraft designed to match these area distributions generally have extremely blunt nose shapes which result in substantial drag. This result, though seemingly paradoxical, can be explained by the created shock-attenuation pattern in which the shock strengths, and therefore the drag, are greatest near the aircraft. Because of special shaping and area growth, secondary shocks from other aircraft components do not overtake and enhance the bow shock during the propagation of the wave front. (See fig. 3.) The net result of this process is weaker shocks at larger distances because of attenuation, but an overall increase in drag. In contrast, notice that the bow shock is weaker on the sharp-nosed aircraft, but coalescence with stronger shocks from rearward components causes a much stronger shock at mid- and far-field distances. If an aircraft configuration is to incorporate boom-minimization features and not suffer aerodynamic penalties which inordinately affect its flight efficiency, range, payload, productivity, and so forth, then means must be provided for including nose-bluntness sensitivity in design trade-off studies.

ANALYSIS

The following is a brief description of the Seebass-George minimization scheme with modifications to provide propagation through the real atmosphere (ref. 7) and control over the bluntness of the area distribution and thereby the drag of the configuration. The assumed form for the class of minimizing F-functions is shown in figure 4. In mathematical terms it may be expressed as:

$$F(y) = 2yH/y_f \qquad (0 \leq y \leq y_f/2) \qquad (2a)$$

$$F(y) = C(2y/y_f - 1) - H(2y/y_f - 2) \qquad (y_f/2 \leq y < y_f) \qquad (2b)$$

$$F(y) = B(y - y_f) + C \qquad (y_f \leq y < \lambda) \qquad (2c)$$

$$F(y) = B(y - y_f) - D \qquad (\lambda \leq y < l) \qquad (2d)$$

In these equations H, B, C, D, and λ are unknown coefficients which are determined by the cruise conditions of the aircraft, by nose length, by the prescribed ratio of bow to rear shock, and by the signature parameter being minimized. Types of signatures studied include flat-topped signatures in which overpressure is minimized with $B = 0$ and signatures in which $F(y)$ is allowed to rise between y_f and λ with a resulting minimum shock followed by a pressure rise as illustrated in figure 4. The value of B in this form of $F(y)$ may range between 0 and S. Recall that the Whitham function $F(y)$ represents the shape characteristics of the pressure signature and is defined in reference 10 and equation (1) in terms of the equivalent area distribution as:

$$F(y) = \frac{1}{2\pi} \int_0^y \frac{A_e''}{(y - \xi)^{1/2}} \, d\xi$$

Crucial to this minimization technique is the fact that equation (1) is an Abel integral equation which may be inverted to give the function A_e in terms of the F-function. When this function is evaluated at l, the result is:

$$A_e(l) = 4 \int_0^l F(y)\,(l - y)^{1/2}\,dy \tag{3}$$

Upon substituting the minimizing form of the F-function into equation (3) and integrating, the following equation for the development of cross-sectional area is obtained:

$$\begin{aligned} A_e(x) = {} & \frac{32}{15}\frac{H}{y_f}x^{5/2} + 1\left(x - \frac{y_f}{2}\right)\frac{8}{15}\left(x - \frac{y_f}{2}\right)^{3/2}\left[\left(\frac{3y_f}{2} + 2x\right)\left(\frac{1}{y_f}\right)(2C - 4H)\right. \\ & \left. + 5(2H - C)\right] + 1(x - y_f)\,4(x - y_f)^{3/2}\left[\left(\frac{2C}{y_f}\right)\left(-\frac{2}{15}\right)(3y_f + 2x) + \frac{2}{3}C\right. \\ & \left. + \frac{4}{15}\left(\frac{H}{y_f}\right)(3y_f + 2x) - \frac{4}{3}H + \frac{2}{15}B(3y_f + 2x) - \frac{2}{3}By_f + \frac{2}{3}C\right] \\ & - 1(x - \lambda)\frac{8}{3}(x - \lambda)^{3/2}(C + D) \end{aligned} \tag{4}$$

where $1(x - l)$ is the Heaviside unit step function. A typical form of the resulting area distribution, A_e, is seen in figure 4.

If the effects of aircraft wake and engine exhaust are neglected, and, if the aircraft cross-section area is zero at its base, then the area at l is entirely due to cruise lift or

$$\begin{aligned} A_e(l) = \frac{W}{\rho u^2} = {} & \frac{32}{15}\frac{H}{y_f}l^{5/2} + \frac{8}{15}\left(l - \frac{y_f}{2}\right)^{3/2}\left[\left(\frac{3y_f}{2}\right) + 2l\left(\frac{1}{y_f}\right)(2C - 4H) + 5(2H - C)\right] \\ & + 4(l - y_f)^{3/2}\left[\left(\frac{2C}{y_f}\right)\left(-\frac{2}{15}\right)(3y_f + 2l) + \frac{2}{3}C + \frac{4}{15}\left(\frac{H}{y_f}\right)(3y_f + 2l) - \frac{4}{3}H\right. \\ & \left. + \frac{2}{15}B(3y_f + 2l) - \frac{2}{3}By_f + \frac{2}{3}C\right] - \frac{8}{3}(l - \lambda)^{3/2}(C + D) \end{aligned} \tag{5}$$

The first constraint imposed upon $F(y)$ is that the front area balance must occur at $y = y_f$, where y_f is the first point at which $F(y) = C$, that is,

$$\int_0^{y_f} F(y)\, dy = G = \frac{\alpha_{yf}}{2} F(y_f) = \frac{\alpha_{yf}}{2} C \tag{6}$$

For the real atmosphere, the advance (ref. 9) of any point of the signal is given by

$$\alpha_y = \frac{\Gamma M_h{}^3 F(y)}{(2\beta)^{1/2}} \int_0^z \frac{p_h}{p}\left(\frac{\rho a_h}{\rho_h a}\right)^{1/2}\left(\frac{A_h}{z_h A}\right)^{1/2} \frac{M}{\beta}\, dz \tag{7}$$

where z is the vertical distance of the signal from the aircraft axis, z_h is the vertical distance of the initial waveform from the aircraft axis, A and A_h are ray-tube areas determined from

$$\frac{A_h}{z_h A} = \left[M_h\left(1 - \frac{1}{M_z{}^2}\right)^{1/2} \int_0^z \frac{dz}{(M_z{}^2 - 1)^{1/2}}\right]^{-1} \tag{8}$$

and $\Gamma = (\gamma + 1)/2$. The initial waveform must be defined away from the aircraft, because the F-function only can represent the body shape accurately at several body lengths away, and the acoustical theory used in describing the propagation of the signal fails near the aircraft. The slope of the balancing line is proportional to the reciprocal of the advance at any point of the signal; thus,

$$S = \frac{(2\beta)^{1/2}}{\Gamma M_h{}^3 \int_0^h \frac{p_h}{p}\left(\frac{\rho a_h}{\rho_h a}\right)^{1/2}\left(\frac{A_h}{z_h A}\right)^{1/2} \frac{M}{\beta}\, dz} = \frac{F(y)}{\alpha_y} \tag{9}$$

For the rear area balancing to occur between points l and y_r, then

$$\int_l^{y_r} F(y)\, dy = \frac{1}{2}\left[B(l - y_f) - D + F(y_r)\right](y_r - l) \tag{10}$$

where y_r is the unknown second intersection point of the rear area balancing line with $F(y)$. If a cylindrical wake is assumed, $F(y)$ and its integral for

$y > l$ can be expressed in terms of $F(y)$ for $y < l$ according to reference 1 as follows:

$$F(y) = -\frac{1}{\pi(y - l)^{1/2}} \int_0^l \frac{(l - \xi)^{1/2}}{y - \xi} F(\xi)\, d\xi \qquad (y > l) \qquad (11)$$

$$\int_l^{y_r} F(y)\, dy = -\frac{2}{\pi} \int_0^l F(\xi) \tan^{-1}\left(\frac{y_r - l}{l - \xi}\right)^{1/2} d\xi \qquad (y > l) \qquad (12)$$

It is necessary to define $F(y)$ and its integral for $y > l$ in this way for optimization problems, since aircraft geometry and thus the Whitham function can be varied arbitrarily only in the range $0 \leq y \leq l$. The constraint on the ratio of shocks is given by

$$\frac{P_f}{P_r} = \frac{C}{D - B(l - y_f) + F(y_r)} \qquad (13)$$

To insure that y_r is an intersection point of $F(y)$ and the balancing line, then

$$F(y_r) = S(y_r - l) + B(l - y_f) - D \qquad (14)$$

and the slope of $F(y)$ at y_r must be less than S.

Solving the system of equations ((5), (6), (10), (13), and (14)) provides values for the constants H, C, D, λ, and y_r. One difficulty of this minimization approach is that, as yet, there is no precise definition of the rise time that will allow the ear to detect only the bow shock and not to be sensitive to the peak as well. With the values of the coefficients known, the minimizing F-function and the area distributions may be determined by equations (2) and (4).

To convert $F(y)$ into pressure near the airplane, the following equation is used:

$$\left(\frac{P}{P_a}\right)_h = \frac{\gamma M^2 F}{(2\beta z_h)^{1/2}} \qquad (15)$$

and on the ground

$$P_g = \left(\frac{A_h}{A_g}\right)^{1/2}\left(\frac{\rho_g a_g}{\rho_h a_h}\right)^{1/2} P_h \tag{16}$$

Finally, by using a ground reflection factor K, the pressure perturbations are converted into the ground signature by

$$\Delta p_g = P_g K \tag{17}$$

The ground-level signature is presented by the signature shown in figure 4.

By taking the limit as $y_f \to 0$ and by using L'Hospital's rule, the expression for area development given above (eq. (4)) reduces to the following delta function form as given by Seebass and George (ref. 6):

$$A_e(x) = 4Gx^{1/2} + \frac{16}{15} Bx^{5/2} + \frac{8}{3} Cx^{3/2} - 1(x - \lambda)\frac{8}{3}(x - \lambda)^{3/2}(C + D) \tag{18}$$

SPECIAL CASES

Special types of pressure signatures occur for large or small values of the weight parameter $\tilde{w}$, where $\tilde{w} = \frac{\beta W}{\rho u^2} \frac{1}{B(l - y_f)^{5/2}}$. These special cases include signatures with no bow shock, signatures with no shocks, and signatures in which the rear shock is less than the bow shock without restriction (fig. 5). Values of $\tilde{w}$ may be checked to indicate when the special calculations are necessary.

No Bow Shock

For no bow shock, the expression for total area reduces to the $y_f = 0$ form (eq. (18)) automatically. Using the facts that $G = \alpha C^2$ and $\lambda = l$ at the minimum length necessary for no shock, the resulting quadratic in C may be solved explicitly to give

$$C = \frac{Bl}{\eta}\left[-\frac{2}{3} \pm \left(\frac{4}{9} - \frac{8\eta}{15} + \frac{\eta}{2}\frac{V}{Bl^{5/2}}\right)\right]^{1/2} \tag{19}$$

where

$$V = \frac{\beta W}{\rho u^2} \qquad B = S\eta \qquad S = \frac{1}{\alpha} \qquad (0 \leq \eta \leq 1) \tag{20}$$

For no bow shock (C = 0) equation (19) reduces to

$$\tilde{w} = \frac{V}{B\ell^{5/2}} \leq \frac{16}{15} \tag{21}$$

in the minimum shock signature.

No Shocks

To eliminate both shock waves, G and C are zero and there must be no discontinuity in F at ℓ. In fact, both F(y) and F'(y) must be continuous at ℓ and thus $A_e'(x)$ and $A_e''(x)$ must be zero there, since A_e is constant for $x > \ell$. With no shocks,

$$A_e(\ell) = \frac{16}{15} B\ell^{5/2} - \frac{8}{3} D(\ell - \lambda)^{3/2} \tag{22}$$

By taking the first and second derivatives and solving the two resulting equations simultaneously

$$\lambda = \frac{2}{3} \ell \tag{23}$$

$$D = \frac{2\eta}{3\alpha} \tag{24}$$

Substituting these values back into the expression for A_e gives

$$\tilde{w} = \frac{V}{B\ell^{5/2}} \leq 0.47407 \tag{25}$$

No Restriction on Rear Shock

Values of $\lambda < \ell$ in the minimizing F-function result because of restrictions on the rear shock. For short lengths, high weights, etc., or other combinations which give large values of $\tilde{w}$, the rear shock is less than the bow shock

without restriction. In these instances $\lambda = l$ and the system of equations is solved without restricting the ratio of rear to front shock:

$$F(y) = \frac{2yh}{y_f} \qquad (0 \leq y \leq y_f/2) \qquad (26a)$$

$$F(y) = C\left(\frac{2y}{y_f} - 1\right) - h\left(\frac{2y}{y_f} - 2\right) \qquad (y_f/2 < y < y_f) \qquad (26b)$$

$$F(y) = B(y - y_f) + C \qquad (y_f/2 \leq y \leq l) \qquad (26c)$$

Substituting this expression for F into equation (3) and integrating gives a quadratic equation in C which can be solved explicitly. Values for C, h, λ, l, and B are now established. For the rear area balance to occur at y_r

$$\int_l^t F(y)\, dy = \frac{1}{2}\left[B(l - y_f) - D + F(y_r)\right](y_r - l) \qquad (27)$$

also, y_r must be an intersection point for $F(y)$ and balance point, or

$$F(y_r) = s(y_r - l) + B(l - y_f) - D \qquad (28)$$

Combining these equations

$$y_r - l = \frac{\int_l^{y_r} F(y)\, dy}{\frac{1}{2}\left[2F(y_r) - S(y_r - 1)\right]} \qquad (29)$$

which may be solved iteratively for y_r with

$$F(y_r) = -\frac{1}{\pi(y_r - l)^{1/2}} \int_0^l \frac{(l - \xi)^{1/2}}{y_r - \xi} F(\xi)\, d\xi \qquad (30)$$

and

$$\int_{l}^{y_r} F(y)\, dy = -\frac{2}{\pi}\int_{0}^{l} F(\xi)\, \tan^{-1}\left(\frac{y_r - l}{l - \xi}\right)^{1/2} d\xi \qquad (31)$$

Substituting back into equation (28) gives the required value for D.

Values of $\tilde{w}$ producing the special cases are shown in figure 5. Typical values giving these extreme $\tilde{w}$'s at M = 2.7, z = 18 288 m (60 000 ft), W = 272 155 kg (600 000 lb) would be l = 33.5 m (110 ft) for no restriction on the rear shock and l = 167.64 m (550 ft) for no bow shock. These values may vary slightly with y_f as seen.

TYPICAL RESULTS

Except as indicated otherwise, all results shown are for the following conditions: Mach number, 2.7; altitude, 18 288 m (60 000 ft); weight, 272 155 kg (600 000 lb); equivalent length, 91.44 m (300 ft); reflection factor, 2.0; ratio of bow to rear shock pressure, 1; and B = 0.58. The value of the front balancing point y_f determines the length of the conical nose region of the equivalent area distribution and is the controlling factor for drag when all of the other flight conditions remain constant. Referring again to figure 4, this position is indicated on the F-function and the corresponding area distribution.

The effect that varying y_f has on the equivalent area distributions for both the minimum-shock and minimum-overpressure signatures is seen in figure 6. Each of the distributions was determined from the inversion formula which defines the effective area corresponding to the minimizing F-function for a given value of y_f. Values of the overpressure and impulse which correspond to these distributions have been inserted for reference. Recall that the impulse is the integral of the positive portion of the pressure signature, as indicated in the signatures at the top of figure 6. Note that the lowest values of overpressure and impulse for these conditions occur when the area distribution has an infinite gradient at the nose. As y_f increases, the longer conical nose region, generated to reduce drag, also causes an increase in overpressure and impulse. Thus, extensive trade-off studies between drag and boom levels would be necessary in any aircraft design studies. The ratio of the increase in overpressure and impulse for both types of signatures as a function of the ratio of nose length to airplane length y_f/l is seen more easily in figure 7. With increasing values of y_f, note that the area under the peak portion of the F-function also increases but not in the same proportions. Therefore, to achieve the necessary total area, the level of the constant portion of the F-function also must increase, thereby producing a higher level of Δp and I. For illustrative purposes, the nose spike of the F-function for $y_f = 0$ has been drawn with a finite width. For this condition, the spike is defined mathematically as a pulse of zero width and infinite height which nevertheless has a finite area. In these figures, Δp is the level of overpressure at the bow shock and represents the initial "bang" heard by the ear when a sonic boom occurs.

The variations of overpressure level and the corresponding drag levels are seen in figure 8. To develop the corresponding variation of drag with y_f, the assumption is made that necessary configuration changes would be confined to the fuselage forebody itself. The increment in drag produced by these changes was calculated using the near-field program of reference 12 and then applied to drag values for a typical arrow-wing SST configuration. As seen in figure 8, there is a sharp decline in drag as the blunt nose is converted to a conical region. Thus, the boom levels could be reduced significantly without prohibitive drag penalties by defining the proper ratio y_f/l.

The actual trend of overpressure with length is seen in figure 9. The lowest curve represents the $y_f = 0$ case, the higher ones increasing with y_f. In all instances observe that overpressure levels decrease with length. Though these results are for minimum-overpressure signatures, similar trends are found to exist for the minimum-shock signatures.

CONCLUDING REMARKS

The analysis for a sonic-boom minimization method has been presented. The method, which represents an extension of previous work, provides the minimizing equivalent area distribution with relaxation of the nose-bluntness requirement for given cruise conditions and includes propagation in the standard atmosphere. The minimizing Whitham F-functions for the minimum-overpressure or minimum-shock signature are also included.

Langley Research Center
National Aeronautics and Space Administration
Hampton, VA 23665
November 13, 1978

APPENDIX

COMPUTER PROGRAM DESCRIPTION AND FLOW CHART

This program calculates the Whitham F-function and the corresponding equivalent area distribution which produce the minimum-overpressure or minimum-shock signature. The solution is based on five governing equations: total area growth (eq. (5)), front area balancing point (eq. (6)), rear area balancing point (eq. (10)), ratio of front to rear shock (eq. (13)), and the area balancing line at the rear balancing point (eq. (14)). These five equations reduce to two nonlinear equations in two unknowns which are solved iteratively using the Newton-Raphson and a combination of the secant and bisection methods.

In calculating the advance of the wave front the standard atmosphere has been used except for an area near the aircraft axis where it is necessary to assume a uniform atmosphere.

This program was coded for the Control Data 6600 computer in Fortran IV. The field length required is 100 000 octal units. Program SEEB is available as LAR 11979 from

COSMIC
Suite 112 Barrow Hall
University of Georgia
Athens, GA 30602

The flow chart of program SEEB is on the following page.

INPUT DESCRIPTION

M	Cruise Mach number (1.25 to 3.0)
Z	Cruise altitude (20 000 to 100 000 ft (6096 to 30 480 m))
L	Airplane equivalent length (200 to 700 ft (60.96 to 213.36 m))
WG	Gross weight of airplane (200 000 to 1 000 000 lb (90 720 to 453 600 kg))
YF	Balancing point in F-function to determine the front shock ($0 \leq y_f/l \leq 0.2$) (Default = 0.0 delta function)
IPRINT	= 0 Iterations on Lambda and T not printed.
	= 1 Iterations printed. (Default = 0)
RKF	Reflection factor. (Default = 2.0)

APPENDIX

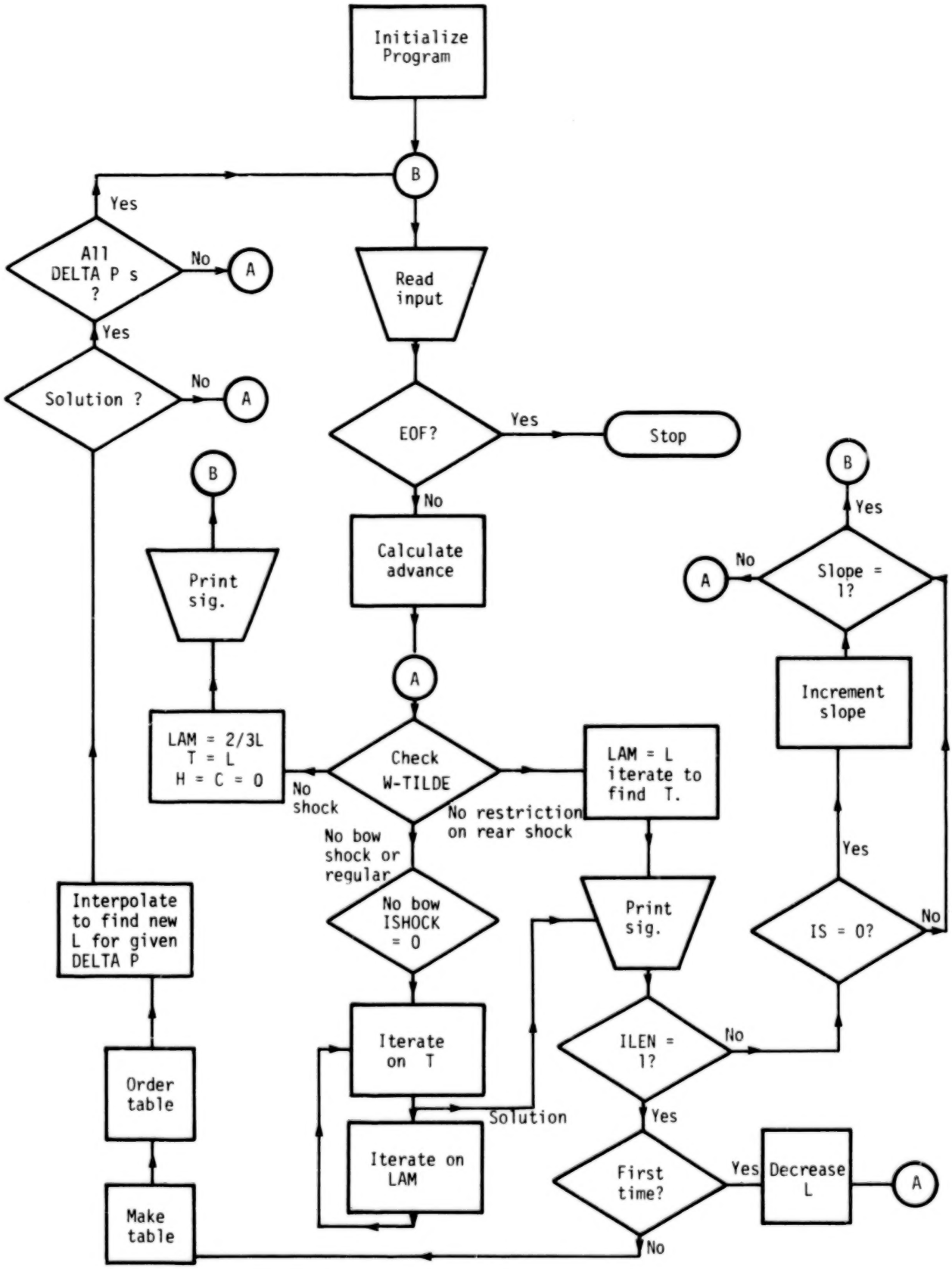
Initialize Program
B
Read input
EOF?
Yes
Stop
No
Calculate advance
A
Check W-TILDE
No shock
No restriction on rear shock
No bow shock or regular
LAM = 2/3L
T = L
H = C = 0
Print sig.
B
LAM = L
iterate to find T.
Print sig.
No bow ISHOCK = 0
Iterate on T
Solution
Iterate on LAM
ILEN = 1?
No
Yes
First time?
Yes
Decrease L
A
No
Slope = 1?
No
A
Yes
B
Increment slope
IS = 0?
Yes
No
All DELTA P s ?
No
A
Yes
Solution ?
No
A
Yes
Interpolate to find new L for given DELTA P
Order table
Make table

BLEN — Factor determining where iteration on T begins. T = BLEN·L
(Default = 3.0)

PRPF — Ratio of rear to front shock
(Default = 1.0)

WIWG — Percentage of gross weight remaining at start of cruise.
W = WIWG·WG (Default = 1.0)

ISIG
= 1 Area, F-function and pressure signature are printed.

= 0 Only the pressure signature is printed.
(Default = 0)

IS
= 0 Minimum-shock and minimum-overpressure signatures.

= 1 Minimum-overpressure signature only.

= 2 Minimum-shock signature only.
(Default = 0)

PERCEN — Factor determining the difference in the slope of the balancing line and the rise portion of the minimum-shock F-function. Slope of rise = Slope of balancing line minus PERCEN times slope of balancing line.
(Default = 0.5)

ICH — Indicates whether the altitude or Mach number changed after the initial run and the advance must be recalculated.

= 0 No change.

= 1 Mach number or altitude did change.
(Default = 0)

ILEN
= 0 Find Δp for given input conditions.

= 1 Iterate to find lengths necessary to give Δp = 0.5, 0.6, 0.7, 0.8, 0.9, and 1.0 psf. A full set of flight conditions including length must be input.
(Default = 0)

IYF
= 0 Delta function used in F-function.

= 1 Nonzero value of y_f used.

If the value of y_f is less than 1, the program automatically uses the delta function in the F-function.
(Default = 1)

APPENDIX

OUTPUT DESCRIPTION

The output consists of a listing of input conditions, the solution coefficients, solution tables, and summary values. Codes exist so that only the pressure signature is printed, the F-function, area, and pressures are printed, or extensive printout occurs during iterations.

The axial position of the front balancing point is y_f.

The advance factor on the ground is α.

Altitude is given in feet and kilometers.

Gross weight is given in pounds.

Cruise weight is given in pounds and kilograms.

WIWG = Ratio of beginning cruise weight to gross weight.

W-TILDE $= \tilde{w} = \dfrac{\beta W}{\rho u^2} \dfrac{\alpha}{\eta (l - y_f)^{5/2}}$

Total Area $= \dfrac{\beta W}{\rho u^2}$

ISLOPE = Code for signature type

0 = Flat-top minimum overpressure

1 = Minimum shock

H, B, C, D, LAM, and y_f are coefficients in equations for F-function and area distribution. (y_r = T; λ = LAM)

X = Axial position for F-function and area distribution near aircraft.

X - BR = $x - \beta z$ = Shifted axial position for pressure signature on the ground.

DELTA P = Δp = Overpressure levels corresponding to $x - \beta z$.

P_1, P_2 = Overpressure levels in pressure signature. P_1 and P_2 at same X - BR indicate a shock.

APPENDIX

SAMPLE CASE

```
$INPUT  M=2.7, Z=60000.0, WG=600000.0, L=300.0, IS=0, ISIG=1, PERCEN=.5,YFL=.1$
```

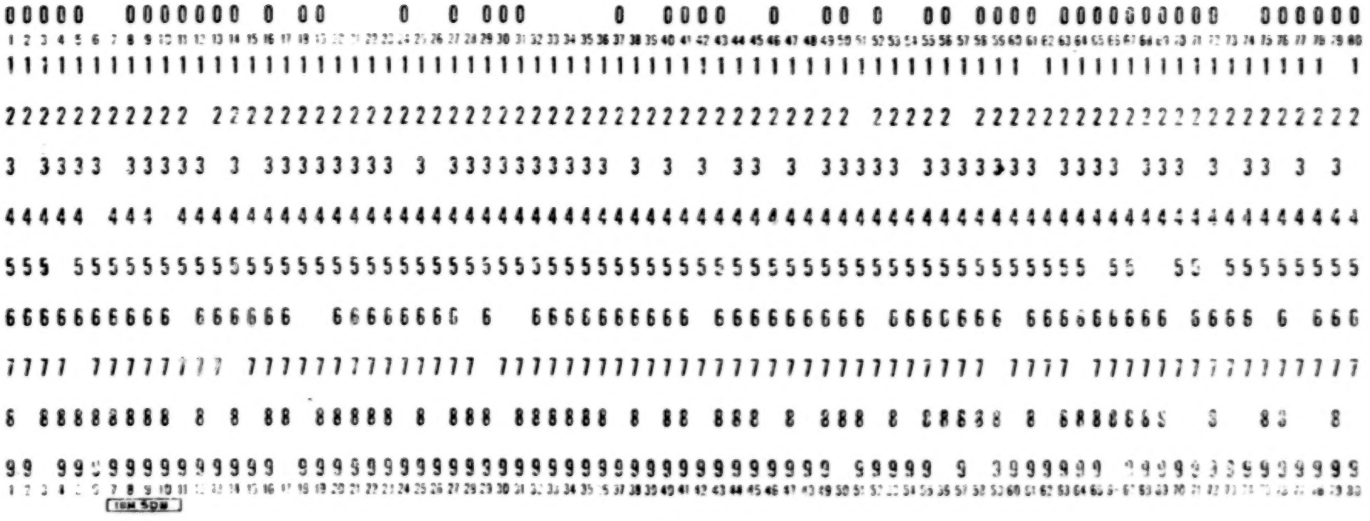

For this sample case an "IS" value of zero was used to produce both a minimum-overpressure solution and a minimum-shock solution.

OUTPUT

MINIMUM-OVERPRESSURE SOLUTION

```
          OVERPRESSURE MINIMIZATION IN REAL ATMOSPHERE AFTER SEEBASS AND GEORGE

POSITIVE VALUE OF YF USED IN F-FUNCTION


     DISTANCE OF INITIAL WAVEFORM FROM AIRCRAFT AXIS IS    .10000000E+04

     THE FRONT BALANCING POINT OCCURS AT AN AXIAL POSITION   OF    .30000000E+02


      THE ADVANCE FACTOR ON THE GROUND IS    .37081361E+04
       CONDITIONS

                MACH NO        =        2.700    REFLECTION FACTOR =        2.000
                ALTITUDE       =    60000.000    EQUIVALENT LENGTH =      300.000
                GROSS WEIGHT   =   600000.000    W-TILDE           =        3.022
                CRUISE WEIGHT  =   600000.000    TOTAL AREA        =      976.263
                WIWG           =        1.000    ISLOPE            =            0

          ALTITUDE=  18.28KILOMETERS    LENGTH=  91.44METERS    WEIGHT=272155.38KILOGRAMS    AREA=  90.69SQUARE METERS

     COEFFICIENTS FOR F FUNCTION AND AREA DISTRIBUTION//

  A=    .34622393E+00
  B=  0.
  C=    .54986270E-01
  D=    .6832420BE-01
  LAM=    .27064490E+03
  T=    .50389657E+03
  YF=    .30000000E+02


  SLOPE OF F(T) AT T =    .50389657E+03     IS   -.10968755E-05
  F(T)=   -.13337939E-01
  SLOPE OF BALANCING LINE=    .26967727E-03
```

MINIMIZING FTAU AND AREA TABLES

	X	F	AREA	X-BR	DELTA P
1	0.	0.	0.		
2	.250000E+01	.577040E-01	.243301E+00		
3	.500000E+01	.115408E+00	.137632E+01		
4	.750000E+01	.173112E+00	.379269E+01		
5	.100000E+02	.230816E+00	.778564E+01		
6	.125000E+02	.288520E+00	.136010E+02		
7	.150000E+02	.346224E+00	.214547E+02		
8	.175000E+02	.297684E+00	.310941E+02		
9	.200000E+02	.249145E+00	.415082E+02		
10	.225000E+02	.200605E+00	.521392E+02		
11	.250000E+02	.152065E+00	.626039E+02		
12	.275000E+02	.103526E+00	.725978E+02		
13	.300000E+02	.549863E-01	.818641E+02	-.173897E+03	.106221E+01
14	.341491E+02	.549863E-01	.957689E+02	-.169748E+03	.106221E+01
15	.382981E+02	.549863E-01	.108821E+03	-.165598E+03	.106221E+01
16	.424472E+02	.549863E-01	.121422E+03	-.161449E+03	.106221E+01
17	.465962E+02	.549863E-01	.133758E+03	-.157300E+03	.106221E+01
18	.507453E+02	.549863E-01	.145938E+03	-.153151E+03	.106221E+01
19	.548943E+02	.549863E-01	.158032E+03	-.149002E+03	.106221E+01
20	.590434E+02	.549863E-01	.170088E+03	-.144853E+03	.106221E+01
21	.631924E+02	.549863E-01	.182140E+03	-.140704E+03	.106221E+01
22	.673415E+02	.549863E-01	.194214E+03	-.136555E+03	.106221E+01
23	.714905E+02	.549863E-01	.206329E+03	-.132406E+03	.106221E+01
24	.756396E+02	.549863E-01	.218500E+03	-.128257E+03	.106221E+01
25	.797886E+02	.549863E-01	.230737E+03	-.124108E+03	.106221E+01
26	.839377E+02	.549863E-01	.243051E+03	-.119959E+03	.106221E+01
27	.880867E+02	.549863E-01	.255448E+03	-.115810E+03	.106221E+01
28	.922358E+02	.549863E-01	.267934E+03	-.111661E+03	.106221E+01
29	.963848E+02	.549863E-01	.280514E+03	-.107512E+03	.106221E+01
30	.100534E+03	.549863E-01	.293191E+03	-.103363E+03	.106221E+01
31	.104683E+03	.549863E-01	.305969E+03	-.992137E+02	.106221E+01
32	.108832E+03	.549863E-01	.318849E+03	-.950646E+02	.106221E+01
33	.112981E+03	.549863E-01	.331834E+03	-.909156E+02	.106221E+01
34	.117130E+03	.549863E-01	.344926E+03	-.867665E+02	.106221E+01
35	.121279E+03	.549863E-01	.358125E+03	-.826175E+02	.106221E+01
36	.125428E+03	.549863E-01	.371432E+03	-.784684E+02	.106221E+01
37	.129577E+03	.549863E-01	.384849E+03	-.743194E+02	.106221E+01
38	.133726E+03	.549863E-01	.398375E+03	-.701703E+02	.106221E+01
39	.137875E+03	.549863E-01	.412012E+03	-.660213E+02	.106221E+01

	X	F	AREA	X-BR	DELTA P
40	.142024E+03	.549863E-01	.425759E+03	-.618722E+02	.106221E+01
41	.146173E+03	.549863E-01	.439616E+03	-.577232E+02	.106221E+01
42	.150322E+03	.549863E-01	.453584E+03	-.535741E+02	.106221E+01
43	.154472E+03	.549863E-01	.467663E+03	-.494251E+02	.106221E+01
44	.158621E+03	.549863E-01	.481852E+03	-.452760E+02	.106221E+01
45	.162770E+03	.549863E-01	.496151E+03	-.411270E+02	.106221E+01
46	.166919E+03	.549863E-01	.510560E+03	-.369779E+02	.106221E+01
47	.171068E+03	.549863E-01	.525079E+03	-.328289E+02	.106221E+01
48	.175217E+03	.549863E-01	.539707E+03	-.286798E+02	.106221E+01
49	.179366E+03	.549863E-01	.554444E+03	-.245308E+02	.106221E+01
50	.183515E+03	.549863E-01	.569290E+03	-.203817E+02	.106221E+01
51	.187664E+03	.549863E-01	.584244E+03	-.162327E+02	.106221E+01
52	.191813E+03	.549863E-01	.599306E+03	-.120836E+02	.106221E+01
53	.195962E+03	.549863E-01	.614475E+03	-.793457E+01	.106221E+01
54	.200111E+03	.549863E-01	.629751E+03	-.378552E+01	.106221E+01
55	.204260E+03	.549863E-01	.645134E+03	.363529E+00	.106221E+01
56	.208409E+03	.549863E-01	.660623E+03	.451258E+01	.106221E+01
57	.212558E+03	.549863E-01	.676218E+03	.866163E+01	.106221E+01
58	.216707E+03	.549863E-01	.691917E+03	.128107E+02	.106221E+01
59	.220856E+03	.549863E-01	.707721E+03	.169597E+02	.106221E+01
60	.225005E+03	.549863E-01	.723630E+03	.211088E+02	.106221E+01
61	.229154E+03	.549863E-01	.739642E+03	.252578E+02	.106221E+01
62	.233303E+03	.549863E-01	.755757E+03	.294069E+02	.106221E+01
63	.237453E+03	.549863E-01	.771974E+03	.335559E+02	.106221E+01
64	.241602E+03	.549863E-01	.788294E+03	.377050E+02	.106221E+01
65	.245751E+03	.549863E-01	.804716E+03	.418540E+02	.106221E+01
66	.249900E+03	.549863E-01	.821238E+03	.460031E+02	.106221E+01
67	.254049E+03	.549863E-01	.837862E+03	.501521E+02	.106221E+01
68	.258198E+03	.549863E-01	.854585E+03	.543012E+02	.106221E+01
69	.262347E+03	.549863E-01	.871409E+03	.584502E+02	.106221E+01
70	.266496E+03	.549863E-01	.888331E+03	.625993E+02	.106221E+01
71	.270645E+03	.549863E-01	.905353E+03	.667483E+02	.106221E+01
72	.270655E+03	-.683242E-01	.905394E+03	.524010E+03	-.131987E+01
73	.271703E+03	-.683242E-01	.909351E+03	.525058E+03	-.131987E+01
74	.272751E+03	-.683242E-01	.913026E+03	.526106E+03	-.131987E+01
75	.273799E+03	-.683242E-01	.916516E+03	.527154E+03	-.131987E+01
76	.274847E+03	-.683242E-01	.919860E+03	.528203E+03	-.131987E+01
77	.275895E+03	-.683242E-01	.923077E+03	.529251E+03	-.131987E+01
78	.276943E+03	-.683242E-01	.926181E+03	.530299E+03	-.131987E+01
79	.277991E+03	-.683242E-01	.929184E+03	.531347E+03	-.131987E+01

	X	F	AREA	X-BR	DELTA P
80	.279039E+03	-.683242E-01	.932093E+03	.532395E+03	-.131987E+01
81	.280087E+03	-.683242E-01	.934915E+03	.533443E+03	-.131987E+01
82	.281135E+03	-.683242E-01	.937654E+03	.534491E+03	-.131987E+01
83	.282183E+03	-.683242E-01	.940316E+03	.535539E+03	-.131987E+01
84	.283231E+03	-.683242E-01	.942905E+03	.536587E+03	-.131987E+01
85	.284279E+03	-.683242E-01	.945423E+03	.537635E+03	-.131987E+01
86	.285327E+03	-.683242E-01	.947874E+03	.538683E+03	-.131987E+01
87	.286375E+03	-.683242E-01	.950260E+03	.539731E+03	-.131987E+01
88	.287424E+03	-.683242E-01	.952585E+03	.540779E+03	-.131987E+01
89	.288472E+03	-.683242E-01	.954849E+03	.541827E+03	-.131987E+01
90	.289520E+03	-.683242E-01	.957055E+03	.542875E+03	-.131987E+01
91	.290568E+03	-.683242E-01	.959205E+03	.543923E+03	-.131987E+01
92	.291616E+03	-.683242E-01	.961301E+03	.544971E+03	-.131987E+01
93	.292664E+03	-.683242E-01	.963343E+03	.546019E+03	-.131987E+01
94	.293712E+03	-.683242E-01	.965334E+03	.547067E+03	-.131987E+01
95	.294760E+03	-.683242E-01	.967275E+03	.548115E+03	-.131987E+01
96	.295808E+03	-.683242E-01	.969166E+03	.549163E+03	-.131987E+01
97	.296856E+03	-.683242E-01	.971010E+03	.550211E+03	-.131987E+01
98	.297904E+03	-.683242E-01	.972806E+03	.551259E+03	-.131987E+01
99	.298952E+03	-.683242E-01	.974557E+03	.552307E+03	-.131987E+01
100	.300000E+03	-.683242E-01	.976263E+03	.553355E+03	-.131987E+01
101	.301000E+03	-.315728E+00		.147176E+04	-.609916E+01
102	.301760E+03	-.246547E+00		.121599E+04	-.476274E+01
103	.302520E+03	-.211033E+00		.108506E+04	-.407668E+01
104	.303280E+03	-.188209E+00		.100118E+04	-.363578E+01
105	.304040E+03	-.171808E+00		.941127E+03	-.331894E+01
106	.304800E+03	-.159203E+00		.995148E+03	-.307545E+01
107	.305560E+03	-.149073E+00		.858345E+03	-.287977E+01
108	.306320E+03	-.140668E+00		.827937E+03	-.271740E+01
109	.307080E+03	-.133526E+00		.802213E+03	-.257942E+01
110	.307840E+03	-.127344E+00		.780047E+03	-.245999E+01
111	.308600E+03	-.121913E+00		.760668E+03	-.235508E+01
112	.309360E+03	-.117084E+00		.743524E+03	-.226180E+01
113	.310120E+03	-.112749E+00		.728208E+03	-.217805E+01
114	.310880E+03	-.108823E+00		.714411E+03	-.210222E+01
115	.311640E+03	-.105243E+00		.701897E+03	-.203307E+01
116	.312400E+03	-.101959E+00		.690477E+03	-.196961E+01
117	.313160E+03	-.989286E-01		.680001E+03	-.191108E+01
118	.313920E+03	-.961201E-01		.670347E+03	-.185683E+01
119	.314680E+03	-.935063E-01		.661414E+03	-.180633E+01

	X	F	AREA	X-BR	DELTA P
120	.315440E+03	-.910646E-01		.653120E+03	-.175916E+01
121	.316200E+03	-.887760E-01		.645393E+03	-.171495E+01
122	.316960E+03	-.866244E-01		.638175E+03	-.167339E+01
123	.317720E+03	-.845963E-01		.631415E+03	-.163421E+01
124	.318480E+03	-.826797E-01		.625068E+03	-.159719E+01
125	.319240E+03	-.808645E-01		.619096E+03	-.156212E+01
126	.320000E+03	-.791416E-01		.613468E+03	-.152884E+01
127	.323678E+03	-.718836E-01		.590232E+03	-.138863E+01
128	.327356E+03	-.659931E-01		.572067E+03	-.127484E+01
129	.331034E+03	-.610636E-01		.557540E+03	-.118000E+01
130	.334712E+03	-.569087E-01		.545737E+03	-.109935E+01
131	.338390E+03	-.533021E-01		.536041E+03	-.102968E+01
132	.342068E+03	-.501467E-01		.528019E+03	-.968723E+00
133	.345746E+03	-.473570E-01		.521352E+03	-.914832E+00
134	.349423E+03	-.448688E-01		.515803E+03	-.866766E+00
135	.353101E+03	-.426328E-01		.511190E+03	-.823571E+00
136	.356779E+03	-.406104E-01		.507368E+03	-.784502E+00
137	.360457E+03	-.387708E-01		.504224E+03	-.748964E+00
138	.364135E+03	-.370890E-01		.501666E+03	-.716476E+00
139	.367813E+03	-.355447E-01		.499618E+03	-.686644E+00
140	.371491E+03	-.341210E-01		.498016E+03	-.659141E+00
141	.375169E+03	-.328037E-01		.496810E+03	-.633695E+00
142	.378847E+03	-.315810E-01		.495954E+03	-.610075E+00
143	.382525E+03	-.304427E-01		.495410E+03	-.588084E+00
144	.386203E+03	-.293800E-01		.495148E+03	-.567556E+00
145	.389881E+03	-.283855E-01		.495138E+03	-.548345E+00
146	.393559E+03	-.274527E-01		.495357E+03	-.530325E+00
147	.397237E+03	-.265758E-01		.495783E+03	-.513365E+00
148	.400914E+03	-.257499E-01		.496399E+03	-.497431E+00
149	.404592E+03	-.249706E-01		.497187E+03	-.482377E+00
150	.408270E+03	-.242340E-01		.498133E+03	-.466147E+00
151	.411948E+03	-.235366E-01		.499225E+03	-.454675E+00
152	.415626E+03	-.228754E-01		.500451E+03	-.441901E+00
153	.419304E+03	-.222475E-01		.501801E+03	-.429772E+00
154	.422982E+03	-.216505E-01		.503265E+03	-.418239E+00
155	.426660E+03	-.210822E-01		.504836E+03	-.407260E+00
156	.430338E+03	-.205405E-01		.506505E+03	-.396796E+00
157	.434016E+03	-.200236E-01		.508266E+03	-.386810E+00
158	.437694E+03	-.195298E-01		.510113E+03	-.377272E+00
159	.441372E+03	-.190576E-01		.512040E+03	-.368150E+00

	X	F	AREA	X-BR	DELTA P
160	.445050E+03	-.186057E-01		.514042E+03	-.359420E+00
161	.448728E+03	-.181727E-01		.516114E+03	-.351055E+00
162	.452406E+03	-.177575E-01		.518253E+03	-.343035E+00
163	.456083E+03	-.173590E-01		.520453E+03	-.335337E+00
164	.459761E+03	-.169763E-01		.522712E+03	-.327944E+00
165	.463439E+03	-.166084E-01		.525026E+03	-.320837E+00
166	.467117E+03	-.162545E-01		.527391E+03	-.314001E+00
167	.470795E+03	-.159138E-01		.529806E+03	-.307420E+00
168	.474473E+03	-.155857E-01		.532267E+03	-.301080E+00
169	.478151E+03	-.152693E-01		.534772E+03	-.294969E+00
170	.481829E+03	-.149642E-01		.537318E+03	-.289075E+00
171	.485507E+03	-.146697E-01		.539904E+03	-.283386E+00
172	.489185E+03	-.143854E-01		.542528E+03	-.277893E+00
173	.492863E+03	-.141106E-01		.545187E+03	-.272585E+00
174	.496541E+03	-.138449E-01		.547880E+03	-.267453E+00
175	.500219E+03	-.135880E-01		.550605E+03	-.262489E+00
176	.503897E+03	-.133393E-01		.553360E+03	-.257685E+00
177	.507575E+03	-.130985E-01		.556146E+03	-.253034E+00
178	.547185E+03	-.109206E-01		.587680E+03	-.210961E+00
179	.586795E+03	-.930342E-02		.621294E+03	-.179721E+00
180	.626406E+03	-.805943E-02		.656291E+03	-.155690E+00
181	.666016E+03	-.707594E-02		.692254E+03	-.136691E+00
182	.705626E+03	-.628120E-02		.728918E+03	-.121339E+00
183	.745237E+03	-.562733E-02		.766103E+03	-.108707E+00
184	.784847E+03	-.508122E-02		.803689E+03	-.981578E-01
185	.824457E+03	-.461923E-02		.841586E+03	-.892333E-01
186	.864068E+03	-.422408E-02		.879731E+03	-.815998E-01
187	.903678E+03	-.388283E-02		.918076E+03	-.750076E-01
188	.943288E+03	-.358563E-02		.956584E+03	-.692663E-01
189	.982899E+03	-.332483E-02		.995228E+03	-.642263E-01
190	.102251E+04	-.309445E-02		.103398E+04	-.597778E-01
191	.106212E+04	-.288969E-02		.107283E+04	-.556224E-01
192	.110173E+04	-.270672E-02		.111177E+04	-.522877E-01
193	.114134E+04	-.254239E-02		.115077E+04	-.491133E-01
194	.118095E+04	-.239415E-02		.118983E+04	-.462496E-01
195	.122056E+04	-.225985E-02		.122894E+04	-.436552E-01
196	.126017E+04	-.213772E-02		.126810E+04	-.412959E-01
197	.129978E+04	-.202625E-02		.130729E+04	-.391427E-01
198	.133939E+04	-.192420E-02		.134653E+04	-.371712E-01
199	.137900E+04	-.183047E-02		.138579E+04	-.353605E-01

	X	F	AREA	X-BR	DELTA P
200	.141861E+04	-.174413E-02		.142508E+04	-.336928E-01
201	.145822E+04	-.166441E-02		.146439E+04	-.321526E-01

PRESSURE SIGNATURE

X-BR	P1	P2
-173.8966	0.0000	1.0622
-169.7475		1.0622
-165.5985		1.0622
-161.4494		1.0622
-157.3004		1.0622
-153.1513		1.0622
-149.0023		1.0622
-144.8532		1.0622
-140.7042		1.0622
-136.5551		1.0622
-132.4061		1.0622
-128.2570		1.0622
-124.1080		1.0622
-119.9589		1.0622
-115.8099		1.0622
-111.6608		1.0622
-107.5118		1.0622
-103.3627		1.0622
-99.2137		1.0622
-95.0646		1.0622
-90.9156		1.0622
-86.7665		1.0622
-82.6175		1.0622
-78.4684		1.0622
-74.3194		1.0622
-70.1703		1.0622
-66.0213		1.0622
-61.8722		1.0622
-57.7232		1.0622
-53.5741		1.0622
-49.4251		1.0622
-45.2760		1.0622
-41.1270		1.0622
-36.9779		1.0622
-32.8289		1.0622
-28.6798		1.0622
-24.5308		1.0622
-20.3817		1.0622
-16.2327		1.0622

X-BR	P1	P2
-12.0836		1.0622
-7.9346		1.0622
-3.7855		1.0622
.3635		1.0622
4.5126		1.0622
8.6616		1.0622
12.8107		1.0622
16.9597		1.0622
21.1088		1.0622
25.2578		1.0622
29.4069		1.0622
33.5559		1.0622
37.7050		1.0622
41.8540		1.0622
46.0031		1.0622
50.1521		1.0622
54.3012		1.0622
58.4502		1.0622
62.5993		1.0622
66.7483		1.0622
524.0104		-1.3199
525.0584		-1.3199
526.1064		-1.3199
527.1545		-1.3199
528.2025		-1.3199
529.2506		-1.3199
530.2986		-1.3199
531.3466		-1.3199
532.3947		-1.3199
533.4427		-1.3199
534.4908		-1.3199
535.5388		-1.3199
536.5868		-1.3199
537.6349		-1.3199
538.6829		-1.3199
539.7310		-1.3199
540.7790		-1.3199
541.8270		-1.3199
542.8751		-1.3199
543.9231		-1.3199

X-BR	P1	P2
544.9711		-1.3199
546.0192		-1.3199
547.0672		-1.3199
548.1153		-1.3199
549.1633		-1.3199
550.2113		-1.3199
551.2594		-1.3199
552.3074		-1.3199
553.3604	-1.3199	-.2577
556.1455		-.2530
587.6799		-.2110
621.2935		-.1797
656.2910		-.1557
692.2544		-.1367
728.9178		-.1213
766.1035		-.1087
803.6888		-.0982
841.5860		-.0892
879.7311		-.0816
918.0760		-.0750
956.5843		-.0693
995.2276		-.0642
1033.9836		-.0598
1072.8347		-.0558
1111.7665		-.0523
1150.7675		-.0491
1189.8282		-.0462
1228.9405		-.0437
1268.0980		-.0413
1307.2950		-.0391
1346.5269		-.0372
1385.7897		-.0354
1425.0799		-.0337
1464.3946		-.0322

FRONT SHOCK = .10622118E+01
REAR SHOCK = .10622118E+01
MAXIMUM PRESSURE= .10622118E+01
W-TILDE = .30221307E+01
LAMBDA/L = .902149b7E+00
IMPULSE= .13922486E+00

```
 (LAM-YF)/(L-YF) =     .89127741E+00
LOCATION OF FRONT SHOCK   -.17389657E+03
LOCATION OF REAR SHOCK     .55335546E+03
TIME BETWEEN SHOCKS     .27823509E+00
CHARACTERISTIC OVERPRESSURE     .20015429E+01

BOW SHOCK= 50.66PA     REAR SHOCK= 50.66PA     MAX PRES= 50.66PA     IMPULSE=  6.67PA-SEC

POSITION OF BOW SHOCK= -53.00METERS     POSITION OF REAR SHOCK= 169.66METERS     CHARACTERISTIC OVERPR=  95.63PA
```

MINIMUM-SHOCK STRENGTH SOLUTION

SHOCK MINIMIZATION IN THE REAL ATMOSPHERE AFTER SEEBASS AND GEORGE

POSITIVE VALUE OF YF USED IN F-FUNCTION

CONDITIONS

MACH NO =	2.700	REFLECTION FACTOR =	2.000
ALTITUDE =	60000.000	EQUIVALENT LENGTH =	300.000
GROSS WEIGHT =	600000.000	W-TILDE =	6.044
CRUISE WEIGHT =	600000.000	TOTAL AREA =	976.263
WIWG =	1.000	ISLOPE =	1

ALTITUDE= 18.288KILOMETERS LENGTH= 91.44METERS WEIGHT=272155.38KILOGRAMS AREA= 90.69SQUARE METERS

FOR THIS MACH NUMBER AND ALTITUDE, THE LENGTH REQUIRED TO ELIMINATE THE BOW SHOCK IS 540.36

THE LENGTH REQUIRED TO ELIMINATE BOTH SHOCKS IS 747.41

RISE TIME SLOPE IS .500 TIMES LOWER THAN SLOPE OF BALANCE LINE

COEFFICIENTS FOR F FUNCTION AND AREA DISTRIBUTION//

H= .30249124E+00
B= .13483863E-03
C= .51533600E-01
D= .10213117E+00
LAM= .25165915E+03
T= .49109360E+03
YF= .30000000E+02

SLOPE OF F(T) AT T = .49109360E+03 IS .69734012E-06
F(T)= -.14191141E-01
SLOPE OF BALANCING LINE= .26967727E-03

MINIMIZING FTAU AND AREA TABLES

	X	F	AREA	X-BR	DELTA P
1	0.	0.	0.		
2	.250000E+01	.504152E-01	.212569E+00		
3	.500000E+01	.100830E+00	.120247E+01		
4	.750000E+01	.151246E+00	.331363E+01		
5	.100000E+02	.201661E+00	.680221E+01		
6	.125000E+02	.252076E+00	.118830E+02		
7	.150000E+02	.302491E+00	.187447E+02		
8	.175000E+02	.260665E+00	.271689E+02		
9	.200000E+02	.218839E+00	.362790E+02		
10	.225000E+02	.177012E+00	.455916E+02		
11	.250000E+02	.135186E+00	.547747E+02		
12	.275000E+02	.933599E-01	.635650E+02		
13	.300000E+02	.515336E-01	.717400E+02	-.161094E+03	.995514E+00
14	.338217E+02	.520489E-01	.831264E+02	-.159183E+03	.100547E+01
15	.376434E+02	.525642E-01	.938973E+02	-.157272E+03	.101542E+01
16	.414651E+02	.530795E-01	.104353E+03	-.155361E+03	.102538E+01
17	.452868E+02	.535949E-01	.114638E+03	-.153450E+03	.103533E+01
18	.491085E+02	.541102E-01	.124839E+03	-.151539E+03	.104529E+01
19	.529303E+02	.546255E-01	.135013E+03	-.149628E+03	.105524E+01
20	.567520E+02	.551408E-01	.145199E+03	-.147718E+03	.106520E+01
21	.605737E+02	.556561E-01	.155428E+03	-.145807E+03	.107515E+01
22	.643954E+02	.561714E-01	.165723E+03	-.143896E+03	.108511E+01
23	.682171E+02	.566867E-01	.176100E+03	-.141985E+03	.109506E+01
24	.720388E+02	.572021E-01	.186574E+03	-.140074E+03	.110502E+01
25	.758605E+02	.577174E-01	.197156E+03	-.138163E+03	.111497E+01
26	.796822E+02	.582327E-01	.207856E+03	-.136252E+03	.112493E+01
27	.835039E+02	.587480E-01	.218681E+03	-.134342E+03	.113488E+01
28	.873256E+02	.592633E-01	.229637E+03	-.132431E+03	.114483E+01
29	.911474E+02	.597786E-01	.240732E+03	-.130520E+03	.115479E+01
30	.949691E+02	.602939E-01	.251969E+03	-.128609E+03	.116474E+01
31	.987908E+02	.608093E-01	.263353E+03	-.126698E+03	.117470E+01
32	.102612E+03	.613246E-01	.274887E+03	-.124787E+03	.118465E+01
33	.106434E+03	.618399E-01	.286575E+03	-.122877E+03	.119461E+01
34	.110256E+03	.623552E-01	.298421E+03	-.120966E+03	.120456E+01
35	.114078E+03	.628705E-01	.310425E+03	-.119055E+03	.121452E+01
36	.117899E+03	.633858E-01	.322592E+03	-.117144E+03	.122447E+01
37	.121721E+03	.639011E-01	.334923E+03	-.115233E+03	.123443E+01
38	.125543E+03	.644165E-01	.347420E+03	-.113322E+03	.124438E+01
39	.129364E+03	.649318E-01	.360085E+03	-.111411E+03	.125434E+01

	X	F	AREA	X-BR	DELTA P
40	.133186E+03	.654471E-01	.372920E+03	-.109501E+03	.126429E+01
41	.137008E+03	.659624E-01	.385926E+03	-.107590E+03	.127425E+01
42	.140830E+03	.664777E-01	.399105E+03	-.105679E+03	.128420E+01
43	.144651E+03	.669930E-01	.412458E+03	-.103768E+03	.129416E+01
44	.148473E+03	.675083E-01	.425987E+03	-.101857E+03	.130411E+01
45	.152295E+03	.680237E-01	.439692E+03	-.999463E+02	.131406E+01
46	.156116E+03	.685390E-01	.453576E+03	-.980354E+02	.132402E+01
47	.159938E+03	.690543E-01	.467638E+03	-.961245E+02	.133397E+01
48	.163760E+03	.695696E-01	.481881E+03	-.942137E+02	.134393E+01
49	.167582E+03	.700849E-01	.496305E+03	-.923028E+02	.135388E+01
50	.171403E+03	.706002E-01	.510911E+03	-.903920E+02	.136384E+01
51	.175225E+03	.711155E-01	.525700E+03	-.884811E+02	.137379E+01
52	.179047E+03	.716308E-01	.540673E+03	-.865703E+02	.138375E+01
53	.182868E+03	.721462E-01	.555831E+03	-.846594E+02	.139370E+01
54	.186690E+03	.726615E-01	.571175E+03	-.827486E+02	.140366E+01
55	.190512E+03	.731768E-01	.586705E+03	-.808377E+02	.141361E+01
56	.194334E+03	.736921E-01	.602423E+03	-.789268E+02	.142357E+01
57	.198155E+03	.742074E-01	.618329E+03	-.770160E+02	.143352E+01
58	.201977E+03	.747227E-01	.634423E+03	-.751051E+02	.144348E+01
59	.205799E+03	.752380E-01	.650708E+03	-.731943E+02	.145343E+01
60	.209620E+03	.757534E-01	.667183E+03	-.712834E+02	.146339E+01
61	.213442E+03	.762687E-01	.683849E+03	-.693726E+02	.147334E+01
62	.217264E+03	.767840E-01	.700707E+03	-.674617E+02	.148330E+01
63	.221085E+03	.772993E-01	.717758E+03	-.655509E+02	.149325E+01
64	.224907E+03	.778146E-01	.735002E+03	-.636400E+02	.150320E+01
65	.228729E+03	.783299E-01	.752440E+03	-.617292E+02	.151316E+01
66	.232551E+03	.788452E-01	.770073E+03	-.598183E+02	.152311E+01
67	.236372E+03	.793606E-01	.787901E+03	-.579074E+02	.153307E+01
68	.240194E+03	.798759E-01	.805925E+03	-.559966E+02	.154302E+01
69	.244016E+03	.803912E-01	.824145E+03	-.540857E+02	.155298E+01
70	.247837E+03	.809065E-01	.842563E+03	-.521749E+02	.156293E+01
71	.251659E+03	.814218E-01	.861179E+03	-.502640E+02	.157289E+01
72	.251669E+03	-.722416E-01	.861227E+03	.519551E+03	-.139555E+01
73	.253395E+03	-.720089E-01	.868764E+03	.520414E+03	-.139105E+01
74	.255121E+03	-.717761E-01	.875575E+03	.521277E+03	-.138655E+01
75	.256847E+03	-.715434E-01	.881927E+03	.522140E+03	-.138206E+01
76	.258574E+03	-.713106E-01	.887914E+03	.523003E+03	-.137756E+01
77	.260300E+03	-.710779E-01	.893592E+03	.523866E+03	-.137307E+01
78	.262026E+03	-.708451E-01	.898999E+03	.524729E+03	-.136857E+01
79	.263752E+03	-.706124E-01	.904162E+03	.525592E+03	-.136407E+01

	X	F	AREA	X-BR	DELTA P
80	.265478E+03	-.703796E-01	.909102E+03	.526455E+03	-.135958E+01
81	.267204E+03	-.701469E-01	.913837E+03	.527318E+03	-.135508E+01
82	.268930E+03	-.699142E-01	.918380E+03	.528181E+03	-.135059E+01
83	.270656E+03	-.696814E-01	.922743E+03	.529044E+03	-.134609E+01
84	.272382E+03	-.694487E-01	.926938E+03	.529907E+03	-.134159E+01
85	.274108E+03	-.692159E-01	.930972E+03	.530771E+03	-.133710E+01
86	.275835E+03	-.689832E-01	.934855E+03	.531634E+03	-.133260E+01
87	.277561E+03	-.687504E-01	.938592E+03	.532497E+03	-.132810E+01
88	.279287E+03	-.685177E-01	.942191E+03	.533360E+03	-.132361E+01
89	.281013E+03	-.682849E-01	.945657E+03	.534223E+03	-.131911E+01
90	.282739E+03	-.680522E-01	.948995E+03	.535086E+03	-.131462E+01
91	.284465E+03	-.678194E-01	.952211E+03	.535949E+03	-.131012E+01
92	.286191E+03	-.675867E-01	.955308E+03	.536812E+03	-.130562E+01
93	.287917E+03	-.673540E-01	.958291E+03	.537675E+03	-.130113E+01
94	.289643E+03	-.671212E-01	.961163E+03	.538538E+03	-.129663E+01
95	.291369E+03	-.668885E-01	.963929E+03	.539401E+03	-.129214E+01
96	.293096E+03	-.666557E-01	.966591E+03	.540264E+03	-.128764E+01
97	.294822E+03	-.664230E-01	.969153E+03	.541127E+03	-.128314E+01
98	.296548E+03	-.661902E-01	.971617E+03	.541990E+03	-.127865E+01
99	.298274E+03	-.659575E-01	.973986E+03	.542853E+03	-.127415E+01
100	.300000E+03	-.657247E-01	.976263E+03	.543716E+03	-.126966E+01
101	.301000E+03	-.269563E+00		.130058E+04	-.520736E+01
102	.301760E+03	-.211841E+00		.108729E+04	-.409229E+01
103	.302520E+03	-.182486E+00		.979203E+03	-.352522E+01
104	.303280E+03	-.163717E+00		.910364E+03	-.316264E+01
105	.304040E+03	-.150264E+00		.861238E+03	-.290276E+01
106	.304800E+03	-.139935E+00		.823699E+03	-.270324E+01
107	.305560E+03	-.131635E+00		.793679E+03	-.254289E+01
108	.306320E+03	-.124742E+00		.768882E+03	-.240974E+01
109	.307080E+03	-.118878E+00		.747897E+03	-.229646E+01
110	.307840E+03	-.113794E+00		.729804E+03	-.219825E+01
111	.308600E+03	-.109320E+00		.713972E+03	-.211181E+01
112	.309360E+03	-.105333E+00		.699950E+03	-.203480E+01
113	.310120E+03	-.101746E+00		.687408E+03	-.196551E+01
114	.310880E+03	-.984903E-01		.676096E+03	-.190261E+01
115	.311640E+03	-.955142E-01		.665820E+03	-.184512E+01
116	.312400E+03	-.927766E-01		.656428E+03	-.179224E+01
117	.313160E+03	-.902449E-01		.647800E+03	-.174333E+01
118	.313920E+03	-.878925E-01		.639837E+03	-.169789E+01
119	.314680E+03	-.856975E-01		.632458E+03	-.165548E+01

	X	F	AREA	X-RR	DELTA P
120	.315440E+03	-.836419E-01		.625595E+03	-.161577E+01
121	.316200E+03	-.817103E-01		.619193E+03	-.157846E+01
122	.316960E+03	-.798898E-01		.613202E+03	-.154329E+01
123	.317720E+03	-.781695E-01		.607583E+03	-.151006E+01
124	.318480E+03	-.765397E-01		.602300E+03	-.147858E+01
125	.319240E+03	-.749924E-01		.597322E+03	-.144869E+01
126	.320000E+03	-.735203E-01		.592623E+03	-.142025E+01
127	.323422E+03	-.676714E-01		.574357E+03	-.130726E+01
128	.326844E+03	-.628157E-01		.559773E+03	-.121346E+01
129	.330266E+03	-.586910E-01		.547900E+03	-.113378E+01
130	.333687E+03	-.551258E-01		.538102E+03	-.106491E+01
131	.337109E+03	-.520017E-01		.529939E+03	-.100456E+01
132	.340531E+03	-.492336E-01		.523096E+03	-.951084E+00
133	.343953E+03	-.467565E-01		.517340E+03	-.903270E+00
134	.347375E+03	-.445283E-01		.512492E+03	-.860186E+00
135	.350797E+03	-.425054E-01		.508413E+03	-.821110E+00
136	.354219E+03	-.406603E-01		.504993E+03	-.785465E+00
137	.357641E+03	-.389688E-01		.502142E+03	-.752790E+00
138	.361062E+03	-.374114E-01		.499789E+03	-.722705E+00
139	.364484E+03	-.359719E-01		.497873E+03	-.694897E+00
140	.367906E+03	-.346366E-01		.496344E+03	-.669102E+00
141	.371328E+03	-.333942E-01		.495158E+03	-.645101E+00
142	.374750E+03	-.322348E-01		.494281E+03	-.622704E+00
143	.378172E+03	-.311500E-01		.493680E+03	-.601748E+00
144	.381594E+03	-.301326E-01		.493330E+03	-.582095E+00
145	.385016E+03	-.291764E-01		.493205E+03	-.563622E+00
146	.388437E+03	-.282757E-01		.493288E+03	-.546223E+00
147	.391859E+03	-.274258E-01		.493558E+03	-.529805E+00
148	.395281E+03	-.266224E-01		.494001E+03	-.514285E+00
149	.398703E+03	-.258617E-01		.494602E+03	-.499589E+00
150	.402125E+03	-.251403E-01		.495348E+03	-.485654E+00
151	.405547E+03	-.244552E-01		.496230E+03	-.472419E+00
152	.408969E+03	-.238036E-01		.497236E+03	-.459833E+00
153	.412391E+03	-.231833E-01		.498357E+03	-.447849E+00
154	.415812E+03	-.225918E-01		.499586E+03	-.436424E+00
155	.419234E+03	-.220274E-01		.500915E+03	-.425520E+00
156	.422656E+03	-.214880E-01		.502337E+03	-.415101E+00
157	.426078E+03	-.209722E-01		.503846E+03	-.405136E+00
158	.429500E+03	-.204784E-01		.505436E+03	-.395596E+00
159	.432922E+03	-.200051E-01		.507103E+03	-.386454E+00

	X	F	AREA	X-BR	DELTA P
160	.436344E+03	-.195512E-01		.508942E+03	-.377686E+00
161	.439766E+03	-.191155E-01		.510649E+03	-.369269E+00
162	.443187E+03	-.186970E-01		.512518E+03	-.361183E+00
163	.446609E+03	-.182945E-01		.514448E+03	-.353409E+00
164	.450031E+03	-.179073E-01		.516434E+03	-.345929E+00
165	.453453E+03	-.175345E-01		.518473E+03	-.338727E+00
166	.456875E+03	-.171753E-01		.520563E+03	-.331788E+00
167	.460297E+03	-.168289E-01		.522701E+03	-.325097E+00
168	.463719E+03	-.164948E-01		.524884E+03	-.318643E+00
169	.467140E+03	-.161723E-01		.527109E+03	-.312412E+00
170	.470562E+03	-.158607E-01		.529376E+03	-.306394E+00
171	.473984E+03	-.155597E-01		.531682E+03	-.300578E+00
172	.477406E+03	-.152685E-01		.534024E+03	-.294954E+00
173	.480828E+03	-.149869E-01		.536401E+03	-.289513E+00
174	.484250E+03	-.147143E-01		.538812E+03	-.284247E+00
175	.487672E+03	-.144503E-01		.541255E+03	-.279147E+00
176	.491094E+03	-.141944E-01		.543729E+03	-.274205E+00
177	.494515E+03	-.139465E-01		.546231E+03	-.269415E+00
178	.535406E+03	-.114628E-01		.577996E+03	-.221821E+00
179	.576297E+03	-.968740E-02		.612219E+03	-.187139E+00
180	.617187E+03	-.832637E-02		.648063E+03	-.160847E+00
181	.658078E+03	-.726300E-02		.685010E+03	-.140305E+00
182	.698969E+03	-.641206E-02		.722745E+03	-.123867E+00
183	.739859E+03	-.571774E-02		.761061E+03	-.110454E+00
184	.780750E+03	-.514194E-02		.799817E+03	-.993308E-01
185	.821641E+03	-.465785E-02		.838913E+03	-.899792E-01
186	.862531E+03	-.424603E-02		.878276E+03	-.820237E-01
187	.903422E+03	-.389209E-02		.917854E+03	-.751865E-01
188	.944313E+03	-.358516E-02		.957607E+03	-.692573E-01
189	.985203E+03	-.331667E-02		.997503E+03	-.640746E-01
190	.102609E+04	-.308070E-02		.103752E+04	-.595122E-01
191	.106698E+04	-.287146E-02		.107763E+04	-.554703E-01
192	.110788E+04	-.268503E-02		.111783E+04	-.518688E-01
193	.114877E+04	-.251805E-02		.115810E+04	-.486431E-01
194	.118966E+04	-.236776E-02		.119844E+04	-.457401E-01
195	.123055E+04	-.223195E-02		.123882E+04	-.431163E-01
196	.127144E+04	-.210869E-02		.127926E+04	-.407351E-01
197	.131233E+04	-.199642E-02		.131973E+04	-.385663E-01
198	.135322E+04	-.189381E-02		.136024E+04	-.365841E-01
199	.139411E+04	-.179973E-02		.140078E+04	-.347667E-01

APPENDIX

	X	F	AREA	X-BR	DELTA P
200	.143500E+04	-.171321E-02		.144135E+04	-.330955E-01
201	.147589E+04	-.163344E-02		.148195E+04	-.315544E-01

PRESSURE SIGNATURE

X-BR	P1	P2
-161.0936	0.0000	.9955
-159.1827		1.0055
-157.2719		1.0154
-155.3610		1.0254
-153.4502		1.0353
-151.5393		1.0453
-149.6285		1.0552
-147.7176		1.0652
-145.8068		1.0752
-143.8959		1.0851
-141.9851		1.0951
-140.0742		1.1050
-138.1633		1.1150
-136.2525		1.1249
-134.3416		1.1349
-132.4308		1.1448
-130.5199		1.1548
-128.6091		1.1647
-126.6982		1.1747
-124.7874		1.1847
-122.8765		1.1946
-120.9657		1.2046
-119.0548		1.2145
-117.1439		1.2245
-115.2331		1.2344
-113.3222		1.2444
-111.4114		1.2543
-109.5005		1.2643
-107.5897		1.2742
-105.6788		1.2842
-103.7680		1.2942
-101.8571		1.3041
-99.9463		1.3141
-98.0354		1.3240
-96.1245		1.3340
-94.2137		1.3439
-92.3028		1.3539
-90.3920		1.3638
-88.4811		1.3738

X-BR	P1	P2
-86.5703		1.3837
-84.6594		1.3937
-82.7486		1.4037
-80.8377		1.4136
-78.9268		1.4236
-77.0160		1.4335
-75.1051		1.4435
-73.1943		1.4534
-71.2834		1.4634
-69.3726		1.4733
-67.4617		1.4833
-65.5509		1.4932
-63.6400		1.5032
-61.7292		1.5132
-59.8183		1.5231
-57.9074		1.5331
-55.9966		1.5430
-54.0857		1.5530
-52.1749		1.5629
-50.2640		1.5729
519.5509		-1.3955
520.4139		-1.3911
521.2770		-1.3866
522.1400		-1.3821
523.0031		-1.3776
523.8661		-1.3731
524.7292		-1.3686
525.5922		-1.3641
526.4553		-1.3596
527.3183		-1.3551
528.1814		-1.3506
529.0444		-1.3461
529.9075		-1.3416
530.7705		-1.3371
531.6336		-1.3326
532.4966		-1.3281
533.3597		-1.3236
534.2227		-1.3191
535.0858		-1.3146
535.9488		-1.3101

X-BR	P1	P2
536.8119		-1.3056
537.6749		-1.3011
538.5380		-1.2966
539.4010		-1.2921
540.2641		-1.2876
541.1271		-1.2831
541.9902		-1.2786
542.8532		-1.2742
543.7285	-1.2697	-.2742
546.2309		-.2694
577.9858		-.2218
612.2190		-.1871
648.0627		-.1608
685.0102		-.1403
722.7455		-.1239
761.0615		-.1105
799.8170		-.0993
838.9125		-.0900
878.2761		-.0820
917.8543		-.0752
957.6068		-.0693
997.5026		-.0641
1037.5174		-.0595
1077.6322		-.0555
1117.8315		-.0519
1158.1030		-.0486
1198.4364		-.0457
1238.8234		-.0431
1279.2569		-.0407
1319.7313		-.0386
1360.2414		-.0366
1400.7832		-.0348
1441.3530		-.0331
1481.9478		-.0316

FRONT SHOCK = .99551394E+00
REAR SHOCK = .99551394E+00
MAXIMUM PRESSURE= .15728875E+01
W-TILDE = .60442614E+01
LAMBDA/L = .83866383E+00
IMPULSE= .14529513E+00

```
 (LAM-YF)/(L-YF) =     .8209596E+00
LOCATION OF FRONT SHOCK   -.1610936E+03
LOCATION OF REAR SHOCK     .5437162E+03
TIME BETWEEN SHOCKS     .2696490E+00
CHARACTERISTIC OVERPRESSURE     .2155321E+01

BOW SHOCK= 47.67PA     REAR SHOCK= 47.67PA     MAX PRES= 75.31PA     IMPULSE=  6.96PA-SEC

POSITION OF BOW SHOCK= -49.10METERS     POSITION OF REAR SHOCK= 165.72METERS     CHARACTERISTIC OVERPR= 103.20PA


DISTANCE FROM BOW SHOCK TO PMAX= 110.83  FEET
TIME FROM BOW SHOCK TO PMAX=     .04  SEC
```

REFERENCES

1. Jones, L. B.: Lower Bounds for Sonic Bangs. J. Roy. Aeronaut. Soc., vol. 65, no. 606, June 1961, pp. 433-436.

2. Jones, L. B.: Lower Bounds for Sonic Bangs in the Far Field. Aeronaut. Q., vol. XVIII, pt. 1, Feb. 1967, pp. 1-21.

3. Seebass, R.: Minimum Sonic Boom Shock Strengths and Overpressures. Nature, vol. 221, no. 5181, Feb. 15, 1969, pp. 651-653.

4. George, A. R.: Lower Bounds for Sonic Booms in the Midfield. AIAA J., vol. 7, no. 8, Aug. 1969, pp. 1542-1545.

5. George, A. R.; and Seebass, R.: Sonic Boom Minimization Including Both Front and Rear Shocks. AIAA J., vol. 9, no. 10, Oct. 1971, pp. 2091-2903.

6. Seebass, R.; and George, A. R.: Sonic-Bcom Minimization. J. Acoust. Soc. America, vol. 51, no. 2 (pt. 3), Feb. 1972, pp. 686-694.

7. Darden, Christine M.: Minimization of Sonic-Boom Parameters in Real and Isothermal Atmospheres. NASA TN D-7842, 1975.

8. Whitham, G. B.: The Flow Pattern of a Supersonic Projectile. Commun. Pure & Appl. Math., vol. V, no. 3, Aug. 1952, pp. 301-348.

9. Walkden, F.: The Shock Pattern of a Wing-Body Combination, Far From the Flight Path. Aeronaut. Q., vol. IX, pt. 2, May 1958, pp. 164-194.

10. Hayes, Wallace D.: Linearized Supersonic Flow. Ph. D. Thesis, California Inst. Technol., 1947.

11. Lung, Joseph Lui: A Computer Program for the Design of Supersonic Aircraft To Minimize Their Sonic Boom. M.S. Thesis, Cornell Univ., 1975.

12. Marconi, Frank; Salas, Manuel; and Yaeger, Larry: Development of a Computer Code for Calculating the Steady Super/Hypersonic Inviscid Flow Around Real Configurations. Volume I - Computational Technique. NASA CR-2675, 1976.

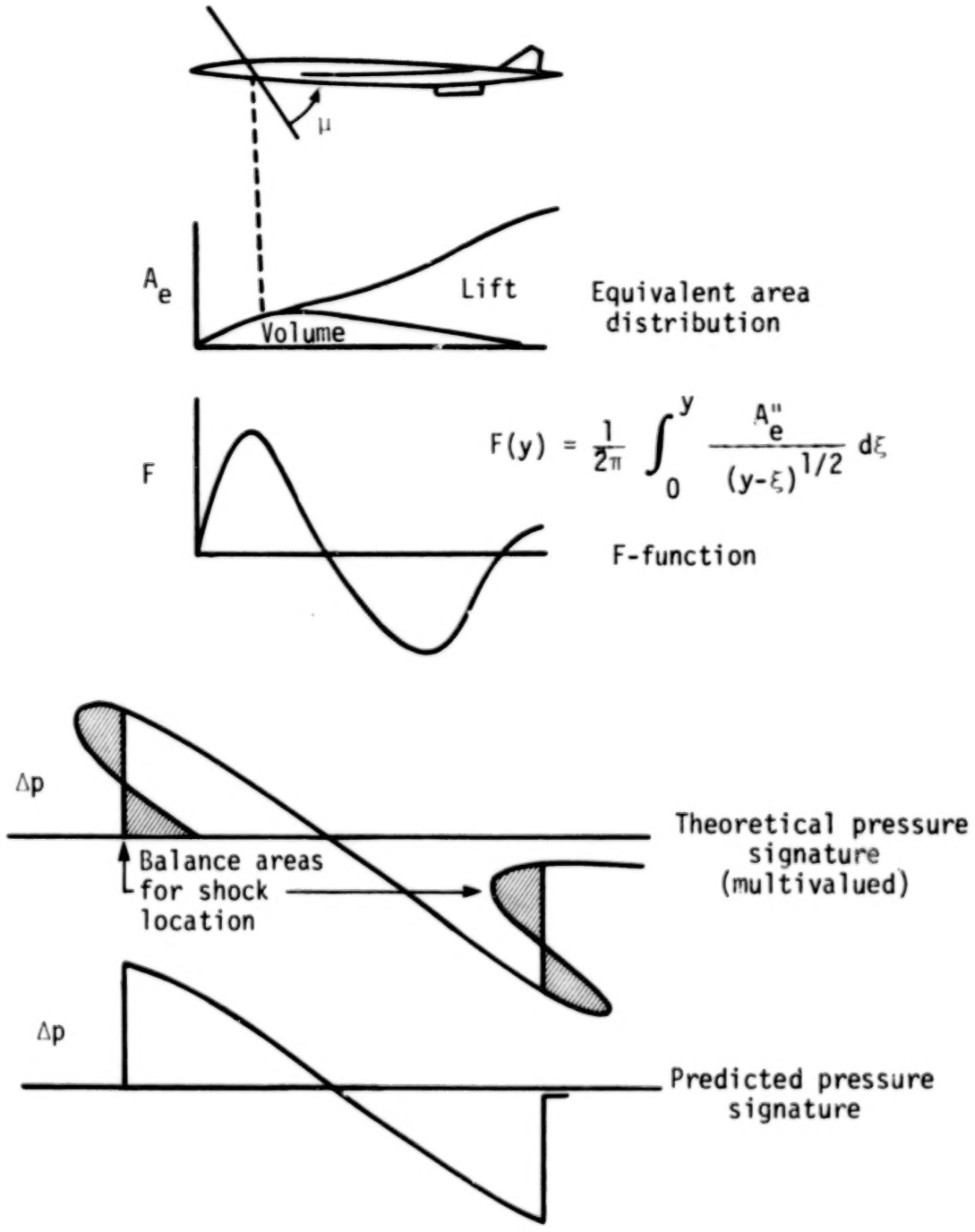

Figure 1.- Sonic-boom prediction methods.

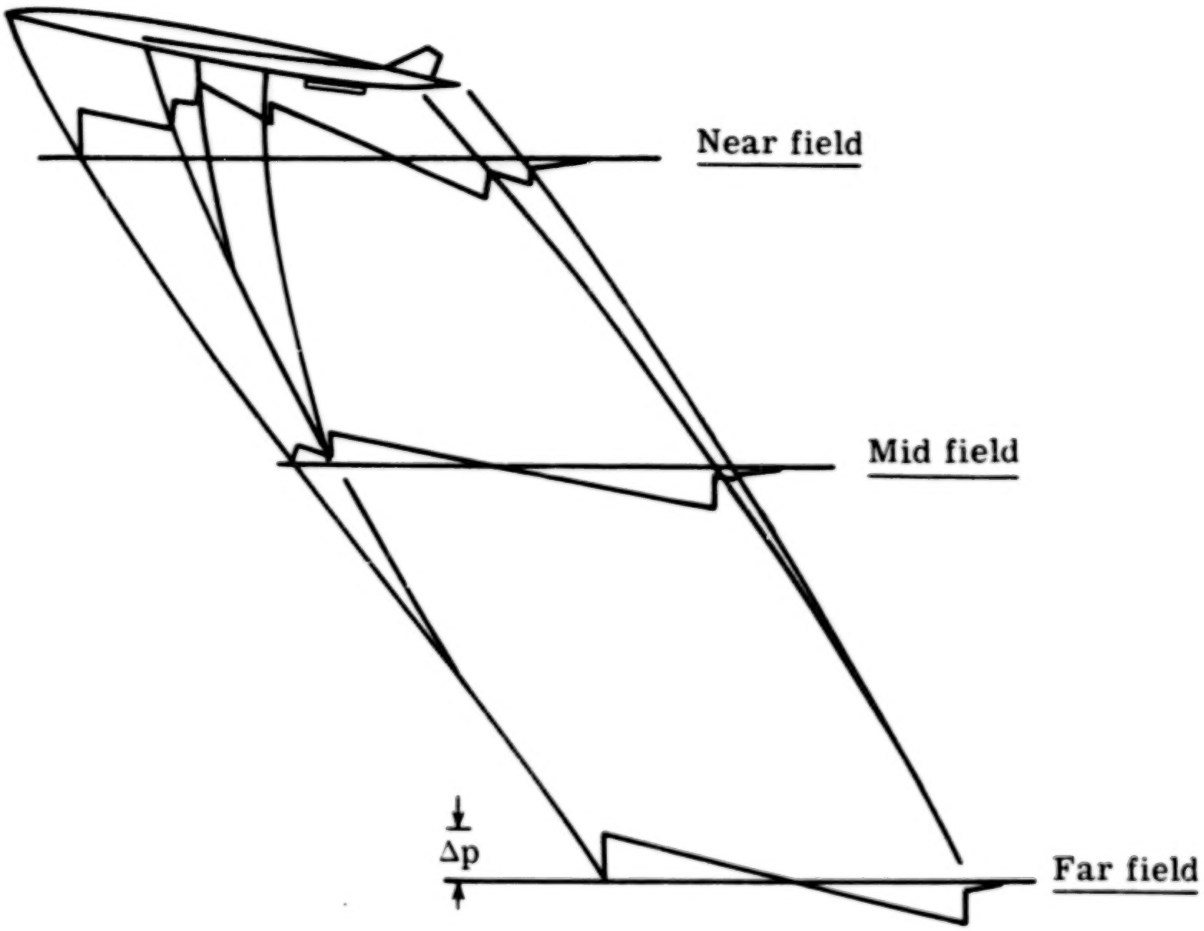

Figure 2.- Pressure-signature propagation.

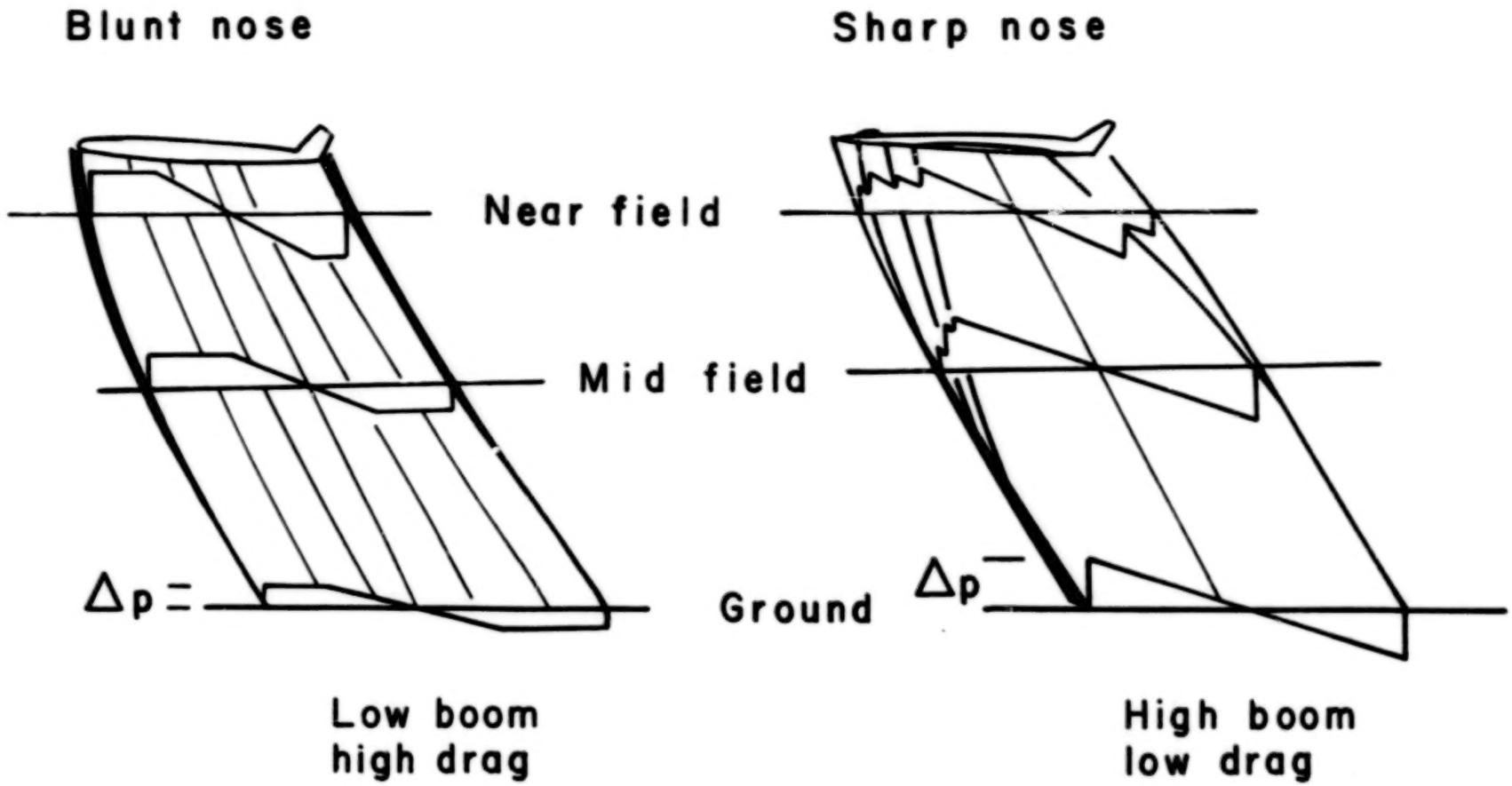

Figure 3.- The low-boom, high-drag paradox.

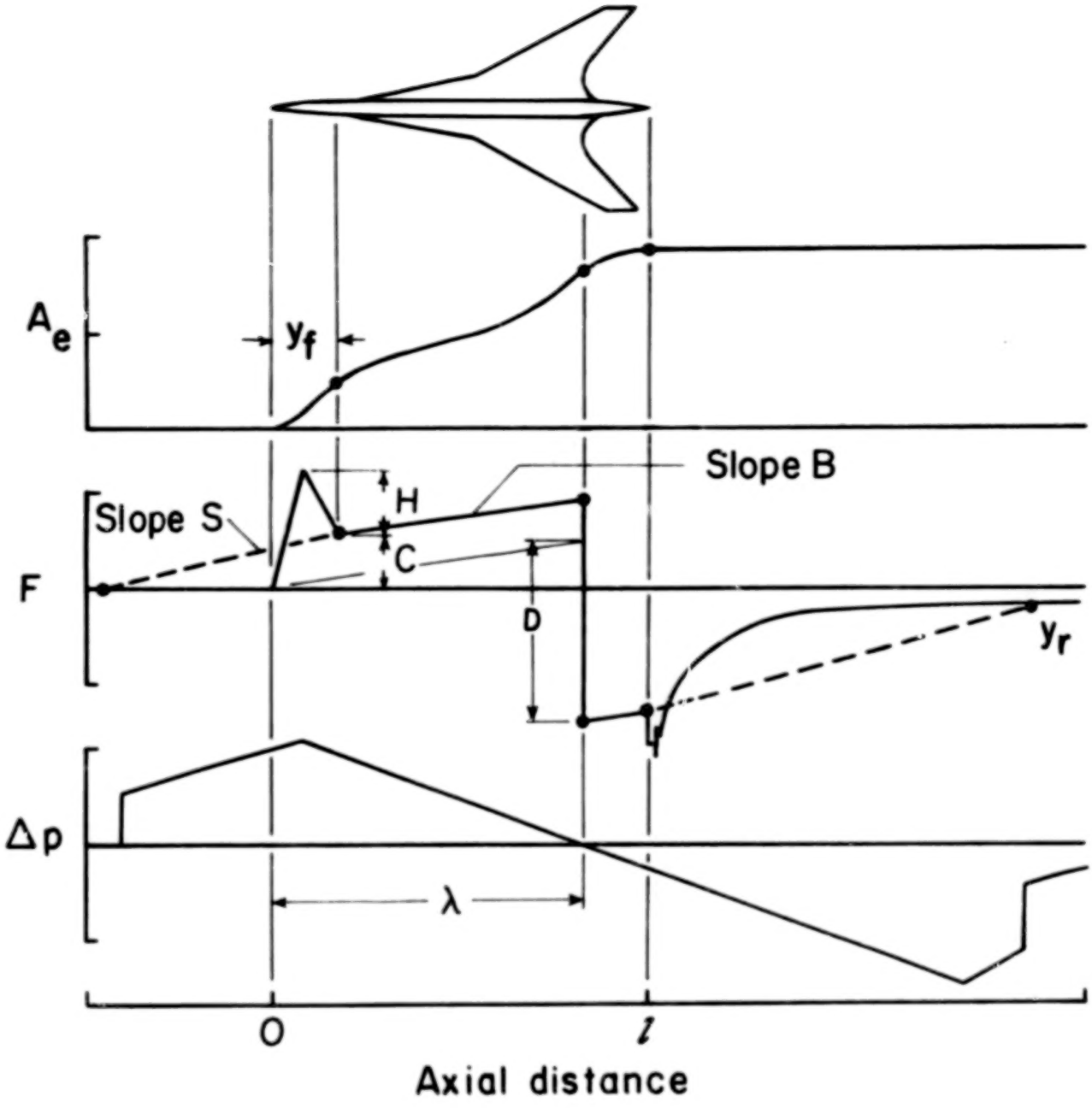

Figure 4.- Illustration of the theoretical concepts of near-field sonic boom.

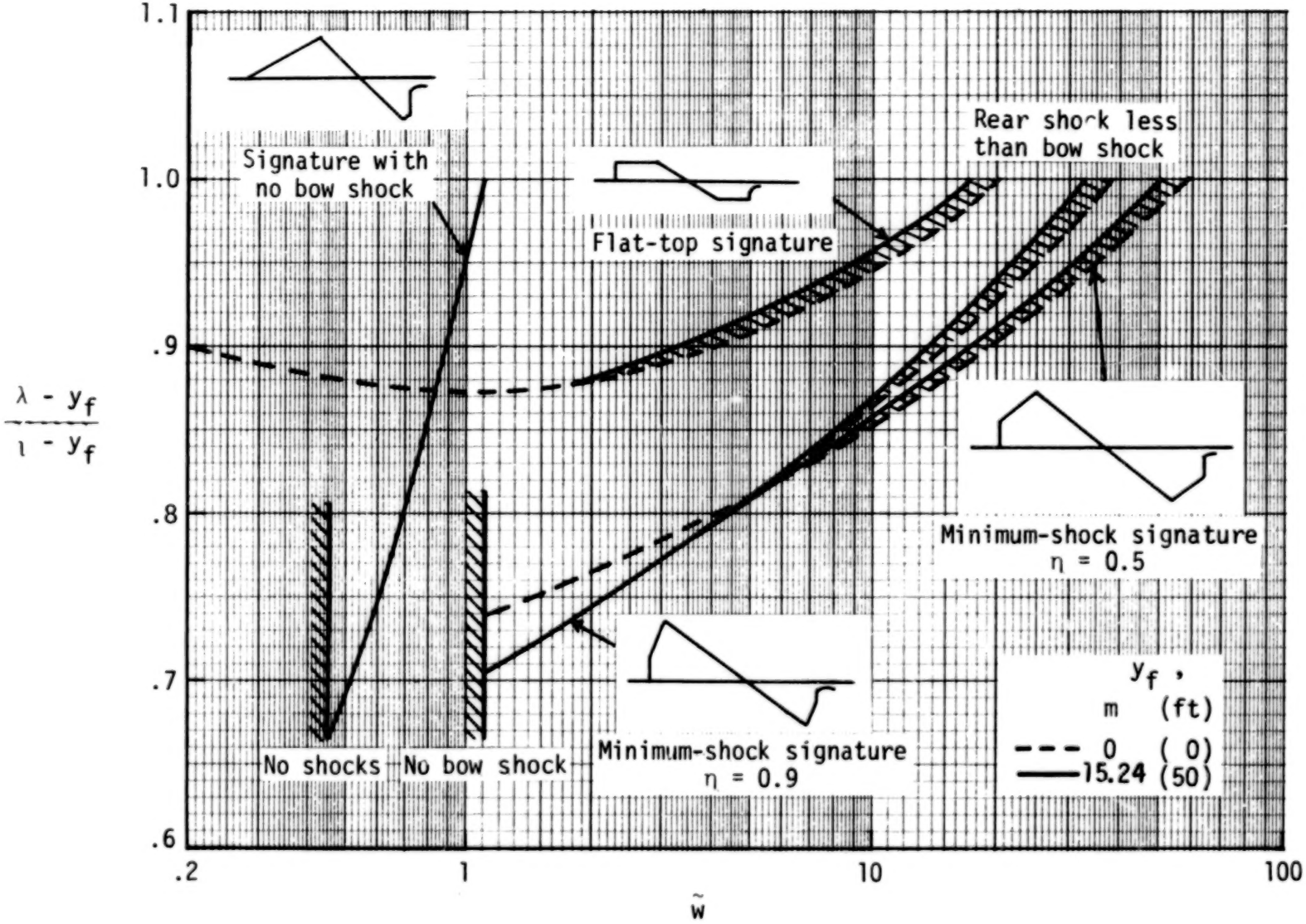

Figure 5.- Special cases shown as function of weight factor.

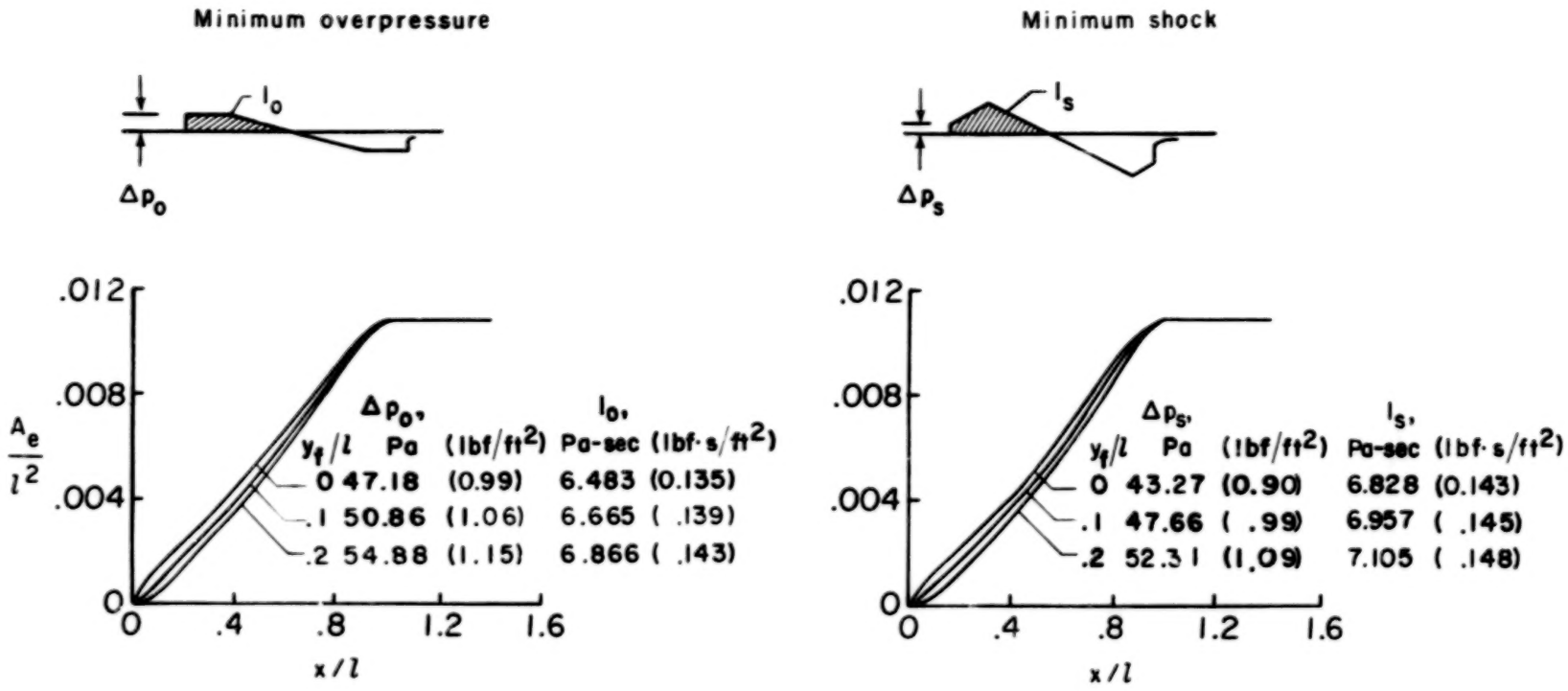

Figure 6.- Typical equivalent-area-distribution requirements for minimization of overpressure and shock.

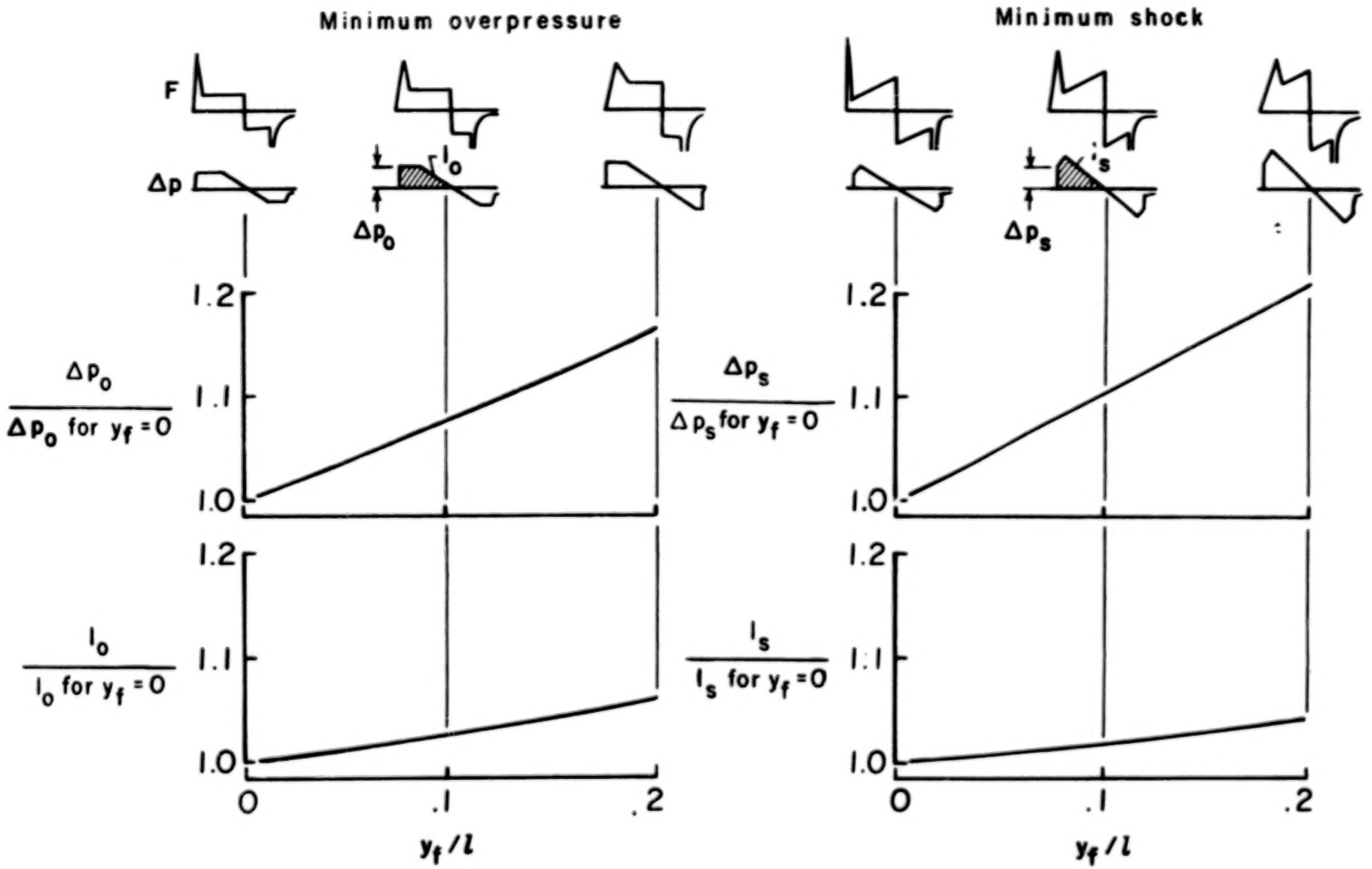

Figure 7.- Variation of shock and impulse with nose length y_f. M = 2.7; h = 18 288 m (60 000 ft); W = 272 155 kg (600 000 lb); l = 91.44 m (300 ft).

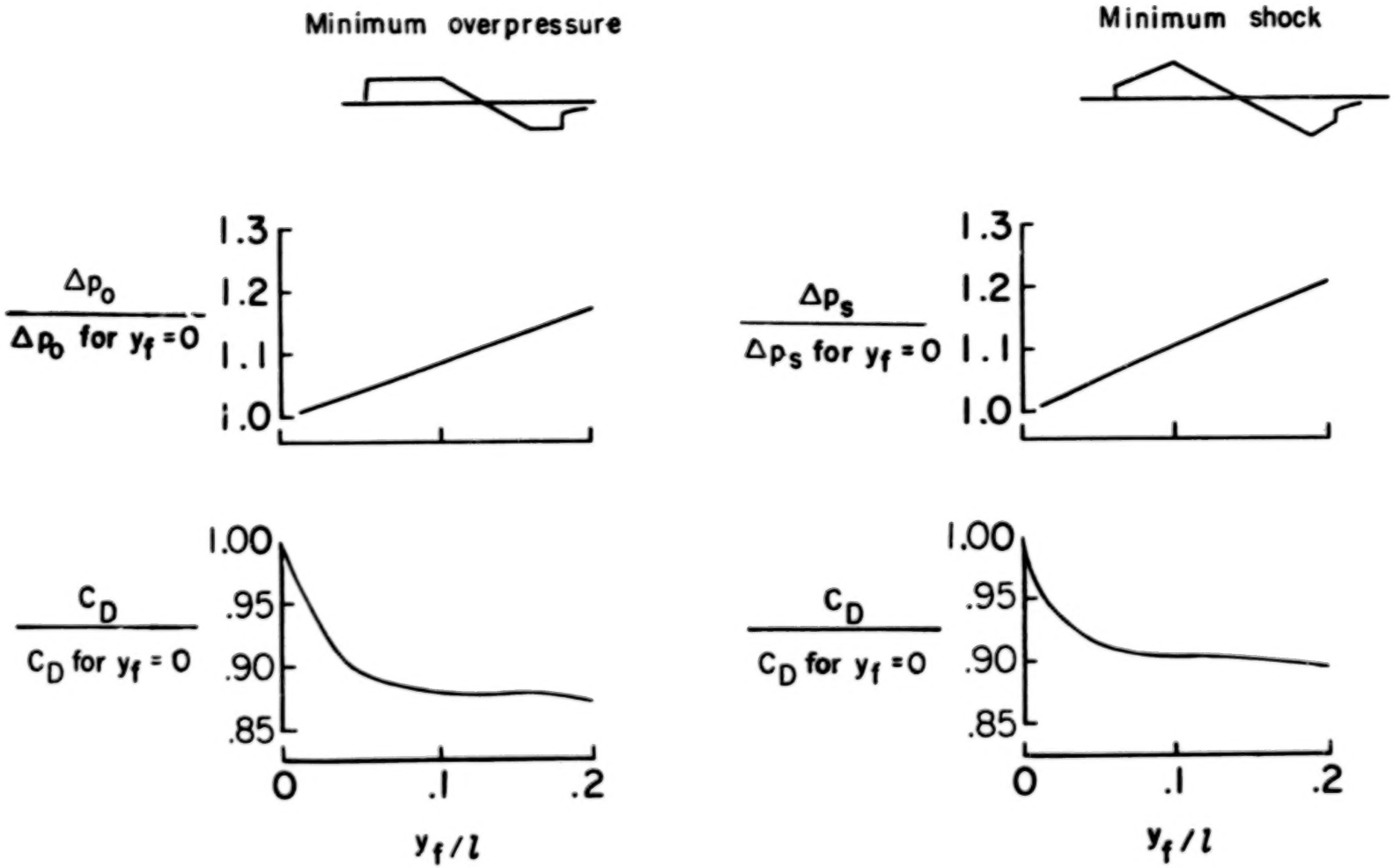

Figure 8.- Estimated drag increments associated with configuration changes for sonic-boom minimization. M = 2.7; h = 18 288 m (60 000 ft); W = 272 155 kg (600 000 lb); l = 91.44 m (300 ft).

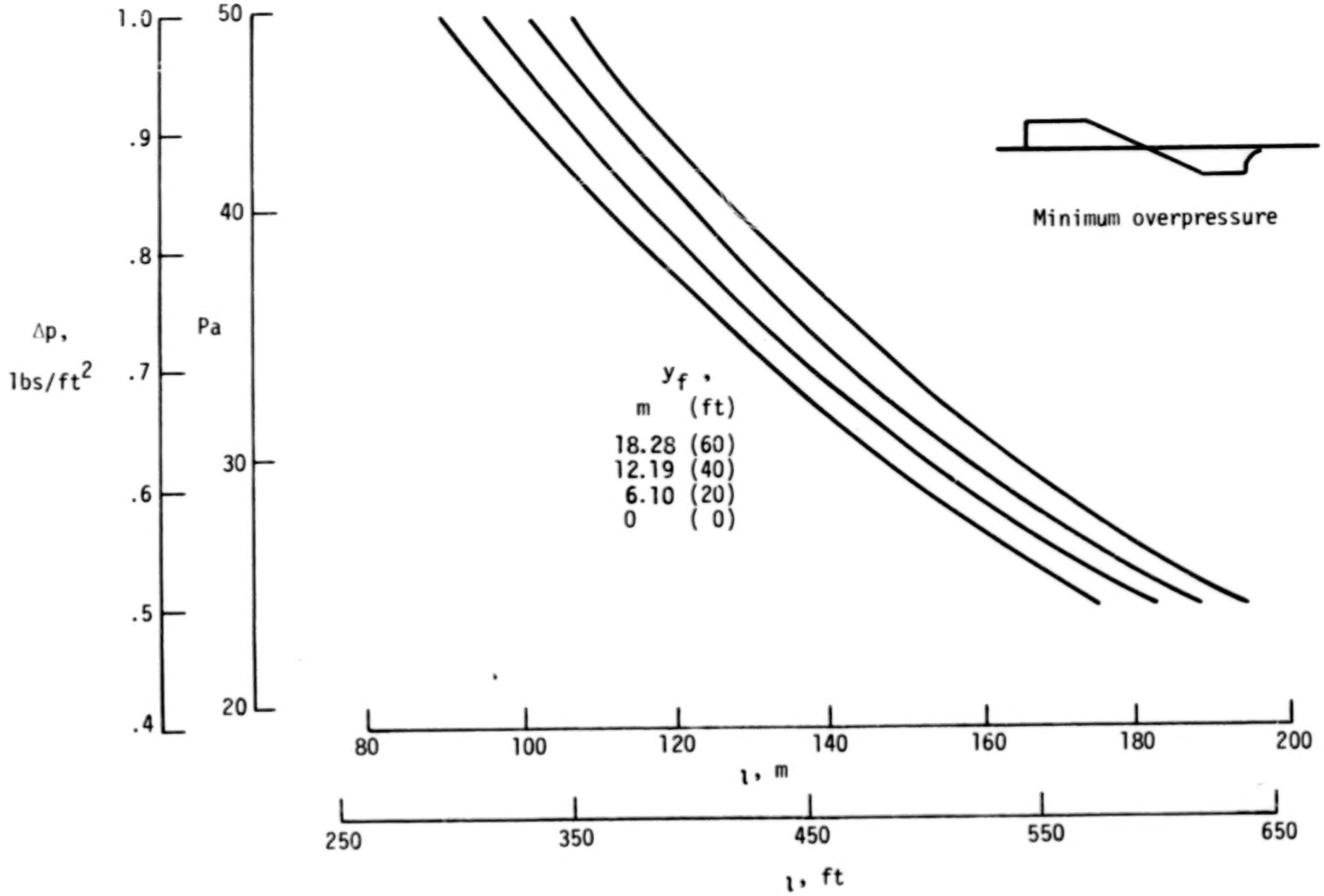

Figure 9.- Overpressure as a function of aircraft length. M = 2.7; W = 272 155 kg (600 000 lb); h = 18 288 m (60 000 ft).

1. Report No.	2. Government Accession No.	3. Recipient's Catalog No.
NASA TP-1348		

4. Title and Subtitle	5. Report Date
SONIC-BOOM MINIMIZATION WITH NOSE-BLUNTNESS RELAXATION	January 1979
	6. Performing Organization Code

7. Author(s)	8. Performing Organization Report No.
Christine M. Darden	L-12464
	10. Work Unit No.
	505-09-23-11

9. Performing Organization Name and Address	11. Contract or Grant No.
NASA Langley Research Center Hampton, VA 23665	
	13. Type of Report and Period Covered
	Technical Paper

12. Sponsoring Agency Name and Address	14. Sponsoring Agency Code
National Aeronautics and Space Administration Washington, DC 20546	

15. Supplementary Notes

16. Abstract

A procedure which provides sonic-boom-minimizing equivalent area distributions for supersonic cruise conditions is described. This work extends previous analyses to permit relaxation of the extreme bluntness required by conventional low-boom shapes and includes propagation in a real atmosphere. The procedure provides area distributions which minimize either shock strength or overpressure.

17. Key Words (Suggested by Author(s))	18. Distribution Statement
Sonic-boom minimization Impulse Pressure signature Equivalent area	Unclassified - Unlimited Subject Category 02

19. Security Classif. (of this report)	20. Security Classif. (of this page)	21. No. of Pages	22. Price*
Unclassified	Unclassified	50	$4.50

* For sale by the National Technical Information Service, Springfield, Virginia 22161

NASA-Langley, 1979

END

APR 30 1979